HUMBOLDT-UNIVERSITÄT ZU BERLIN

MATHEMATISCH-NATURWISSENSCHAFTLICHE FAKULTÄT I

INSTITUT FÜR BIOLOGIE

Bachelorarbeit

ZUM ERWERB DES AKADEMISCHEN GRADES

BACHELOR OF SCIENCE

„Theoretische und computergeschützte Analyse negativer Rückkopplungsmechanismen sowie der Dosis-Wirkungs-Beziehung im Pheromon Signalweg in der Bäckerhefe Saccharomyces cerevisiae“

„Theoretical and computational analysis of negative feedback mechanisms and the dose-response alignment in the pheromone signalling pathway of the yeast Saccharomyces cerevisiae “

vorgelegt von

Adriana Supady

geb. am 25.07.1987 in Olsztyn (Polen)

angefertigt in der Arbeitsgruppe Theoretische Biophysik

am Institut für Biologie

Berlin, im September 2009

Abstract

In order to transmit information about the presence of the pheromone and to respond distinguishably to different pheromone concentrations the yeast *Saccharomyces cerevisiae* uses a cell signalling system. The MAP Kinase Fus3 mediates a negative feedback that improves the accuracy of the information transmission. In this thesis four possible models with different incorporated feedbacks are proposed and analysed. Furthermore, the results of parameter estimations and the predictions of the models are discussed.

Zusammenfassung

Die Bäckerhefe *Saccharomyces cerevisiae* benutzt einen zellulären Signalweg um die Information über die Existenz von Pheromonen weiterzuleiten und um differenzierbar auf verschiedene Pheromonkonzentrationen zu reagieren. Die MAP-Kinase Fus3 vermittelt eine negative Rückkopplung, die für die Genauigkeit der Informationsweiterleitung verantwortlich ist. Insgesamt werden in dieser Arbeit vier ausführbare Modelle mit verschiedenen Rückkopplungsmechanismen vorgeschlagen und analysiert. Weiterhin werden die Resultate der Parameterschätzung und die Vorhersagen der Modelle diskutiert.

Contents

1 Introduction 6
1.1 Objective 6
1.2 Signalling pathways in *Saccharomyces cerevisiae* 6
1.3 Pheromone signalling pathway in *Saccharomyces cerevisiae* 8
1.3.1 G protein cycle activation 8
1.3.2 The scaffold-dependent MAPK pathway 9
1.3.3 Downstream effects of activated Fus3 9
1.4 Initial dynamics of the system 10
1.5 Dose-response alignment 11
2 Theoretical background & methods 14
2.1 Mathematical modelling of reaction networks with ODE systems. 14
2.2 Parameter estimation 15
2.3 Model selection and Akaike's Information Criterion (AIC) 16
2.4 Parameter Sensitivity Analysis 17
3 Data 19
3.1 Data plots 19
3.2 Discussion of the data 22
4 Model construction 25
4.1 Model A 26
4.2 Model B 27
4.3 Model C 28
4.4 Model D 29
5 Results 30
5.1 Results of parameter estimation 30
5.1.1 Model A 31
5.1.2 Model B 32
5.1.3 Model C 33
5.1.4 Model D 34
5.1.5 Results of parameter estimation – summary 35
5.2 Model selection 36
5.3 Predictions of the model: dose -response alignment 36
5.4 Parameter sensitivity analysis 40
6 Discussion 42
6.1 Parameter estimation 42
6.2 Model selection 43
6.3 Predictions of the model 43
6.4 Conclusion 44
7 Outlook 45
8 References 46
Acknowledgments 51

List of Figures

Figure 1.1: Overview of signalling pathways in yeast 7
Figure 1.2: All system responses (a,b,c). 10
Figure 1.3: Dose responses of receptor occupancy and pathway output align closely. 11
Figure 1.4: Dose-response alignment 12
Figure 1.5: Dose responses of receptor occupancy and pathway output do not align. 12
Figure 1.6: Dose-response misalignment. 13
Figure 3.1: Fus3 phosphorylation (fus3-as2) 19
Figure 3.2: Fus3 phosphorylation (kss1-as2) 20
Figure 3.3: Ste5 membrane recruitment (fus3-as2) 20
Figure 3.4: G-protein dissociation (fus3-as2) 21
Figure 3.5: Ste5 membrane recruitment (fus3-as2 Δsst2) 21
Figure 3.6: Ste5 membrane recruitment (fus3-as2 sst2 T134A) 22
Figure 4.1: The common part of all model structures - Model 0 25
Figure 4.2: The structure of Model A 26
Figure 4.3: The structure of Model B 27
Figure 4.4: The structure of Model C 28
Figure 4.5: The structure of Model D 29
Figure 5.1: Results of parameter estimation: Model A. 31
Figure 5.2: Results of parameter estimation: Model B. 32
Figure 5.3: Results of parameter estimation: Model C. 33
Figure 5.4: Results of parameter estimation: Model D. 34
Figure 5.5: Model B: the disruption of the dose-response alignment 38
Figure 5.6: Model C: the disruption of the dose-response alignment. 38
Figure 5.7: Predictions of the Model B compared with experimental data 39
Figure 5.8: Predictions of the Model C compared with experimental data 39

List of Tables

Table 5.1: The calculated values of AIC 36
Table 5.2: Calculated values of reduction of EC_{50}. 37
Table 5.3: Calculated values of correlation coefficients. 39
Table 5.4: Calculated sensitivities 40

1 Introduction

1.1 Objective

The objective of this thesis is to propose a simplified model of a negative feedback mechanism in pheromone signalling pathway in yeast as well as to discuss the existence of dose-response alignments in the system.

The dose-response alignment is a proportional relationship between receptor occupancy and downstream response of the signalling pathway. It was revealed that the dose-response alignment is a result of a negative feedback mediated by mitogen-activated protein kinase Fus3 [Yu *et al.* 2008]. Active Fus3 negatively regulates one of the functions of Sst2, one of the principal regulators of mating pheromone signalling in yeast. It was also suggested that the negative feedback could be a mechanism responsible for the fidelity of information transmission also in other biological systems [Yu *et al.* 2008].

1.2 Signalling pathways in *Saccharomyces cerevisiae*

Signal transduction pathways enable cells to respond to external stimuli through sensing and transmission of the signals within the cell, as well as through initializing changes in the cell. The accurate functioning of these pathways is required for adaption and survival of the cells under various conditions [Klipp & Liebermeister 2006]. Although there are many kinds of signalling pathways, they possess similar building modules (receptors, G-protein cycles, mitogen activated protein kinase (MAPK) cascades). There exist many interactions between the pathways (crosstalk) that lead to forming a network. The Yeast *Saccharomyces cerevisiae* possess several signalling pathways, e.g.: HOG pathway, pheromone pathway, pseudohyphal growth pathway and glucose sensing pathway (Figure 1.1). The high osmolarity glycerol (HOG) pathway is activated by osmotic shock (an increase in environmental osmolarity) and results in the production of

glycerol concentration to prevent the dehydration of the cell [Hayashi & Maeda 2006]. The pheromone signalling pathway is activated by the binding of extracellular pheromone to the receptor and can result in a polarized cell growth, transcription of new genes and arrest of the cell cycle in order to prepare to cell fusion and diploid formation [Shao *et al.* 2006]. The pseudehyphal growth pathway is activated in case of nitrogen starvation and results in dimorphic transition of the cells known as pseudohyphal differentiation [Lorenz & Heitman 1997]. The glucose sensing pathway is activated in the presence of extracellular glucose and results in various changes of cellular metabolism in the yeast cells [Nazarko et al. 2007].

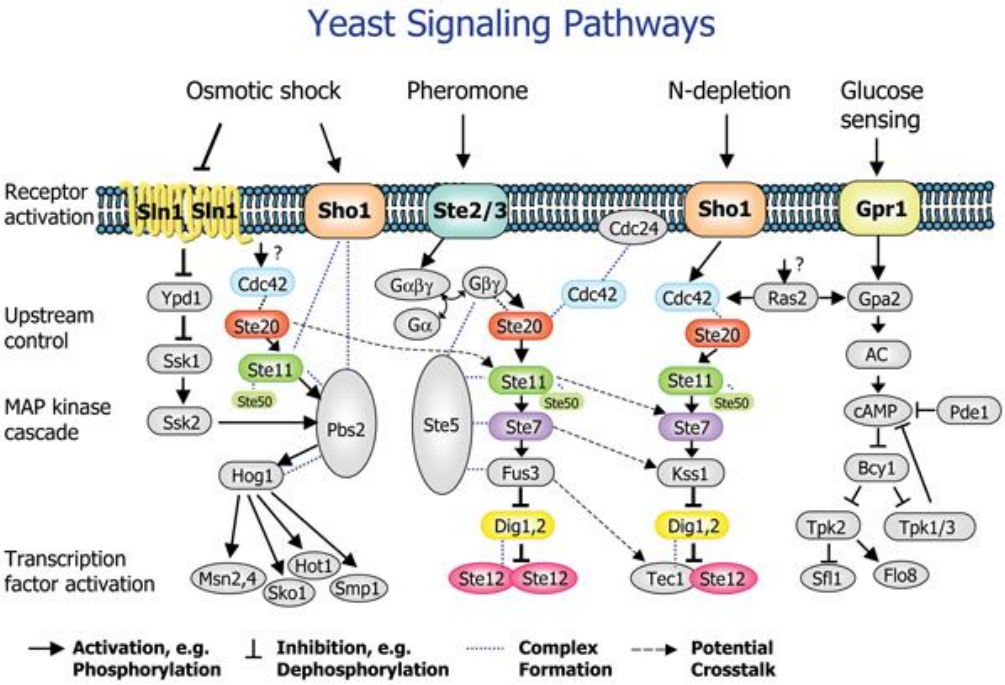

Figure 1.1: Overview of signalling pathways in yeast
[Klipp & Liebermeister 2006]

1.3 Pheromone signalling pathway in *Saccharomyces cerevisiae*

The yeast pheromone pathway is one of the best understood and described pathways in eukaryotes [Drogen van *et al.* 2001, Kofahl & Klipp 2004, Wang & Dohlman 2004, Qi & Elion 2005, Klipp & Liebermeister 2006, Schaber *et al*. 2006, Shao *et al.* 2006]. This pheromone signalling system can be divided into three modules: G-protein cycle activation, the MAPK cascade and the downstream effects of activated Fus3.

1.3.1 G protein cycle activation

There are two types of haploid cells in budding yeast *Saccharomyces cerevisiae*: MATα cells which secrete α-factor and MATa cells which secrete a-factor. These factors are mating signals, small peptide pheromones responsible for binding to a cell surface receptor Ste2 (in MATa cells; Ste3 in MATα cells) and cause its activation. The activated receptor can be deactivated, internalized or interact with the subunit Gα of G-protein. The G-protein is a heterotrimer consisting of three subunits: Gα, Gβ and Gγ. The interaction of Gα with the activated receptor leads to conformational changes that result in a release of GDP and binding to GTP by the Gα subunit and in a dissociation of the G protein into GαGTP subunit and a heterodimer G$\beta\gamma$. The GαGTP subunit can be hydrolized and return into initial state GαGDP. As a consequence, GαGDP can reassociate with G$\beta\gamma$ into the heterotrimer and close the cycle. Regulators of G protein signalling (RGS proteins) can accelerate the hydrolization of GαGTP. The principal regulator is Sst2 that interacts with GαGTP and increase its GTPase activity [Chasse *et al.* 2006, Hao *et al.* 2003].

1.3.2 The scaffold-dependent MAPK pathway

During the G protein cycle, the released heterodimer Gβγ can bind and activate other components of the pathway. The most essential step in the pheromone signal transmission is the ability of Gβγ to bind to the scaffold protein Ste5. The function of a scaffold protein is to localise and tether all required components in one particular area in the cell as well as to coordinate the feedbacks [Shaw & Filbert 2009]. Afterwards Ste5 recruits Ste11 to the plasma membrane and activates the MAPK cascade. The first step in the cascade is the phosporylation of the serine and threonine residues in the N-terminal kinase region of MAPKKK Ste11 by a membrane-associated kinase Ste20 resulting in Ste11 activation. The activated Ste11 phosporylates the MAPKK Ste7 and activates it in this way. Analogically, the activated Ste7 activates two other MAPKs: Fus3 and Kss1. More relevant for the mating process is the Fus3, while Kss1 is responsible for the invasive growth of the cell and is also dependent on osmotic stress. The Ste7-dependent activation of Fus3 takes place by phosporylation of threonine and tyrosine residues in the activating loop. After double-phosporylation, activated Fus3 rapidly dissociates from the scaffold protein Ste5. The Ste5 remains tethered to the plasma membrane acting as platform and enables phosporylation of many Fus3 molecules.

1.3.3 Downstream effects of activated Fus3

The double phospohorylated MAPK Fus3 is responsible for phosporylation of various proteins: Far1 (bifunctional scaffold protein, responsible for morphological changes and the arrest of the cell cycle), Ste12 (transcriptional activator responsible for the expression of pheromone-induced genes), Dig1/Rst1 & Dig2/Rst2 (repressors acting by binding to the Ste12) and Sst2 (RGS protein,

responsible for the acceleration of the GαGTP hydrolization). The most crucial for this model is the phosporylation of Sst2.

In this thesis only the downstream effects that take place within first 15 minutes are considered.

1.4 Initial dynamics of the system

The initial system dynamics are presented with the help of experimental data. The data were presented in [Yu *et al.* 2008]. System outputs were measured after stimulating cells with 100 nM pheromone.

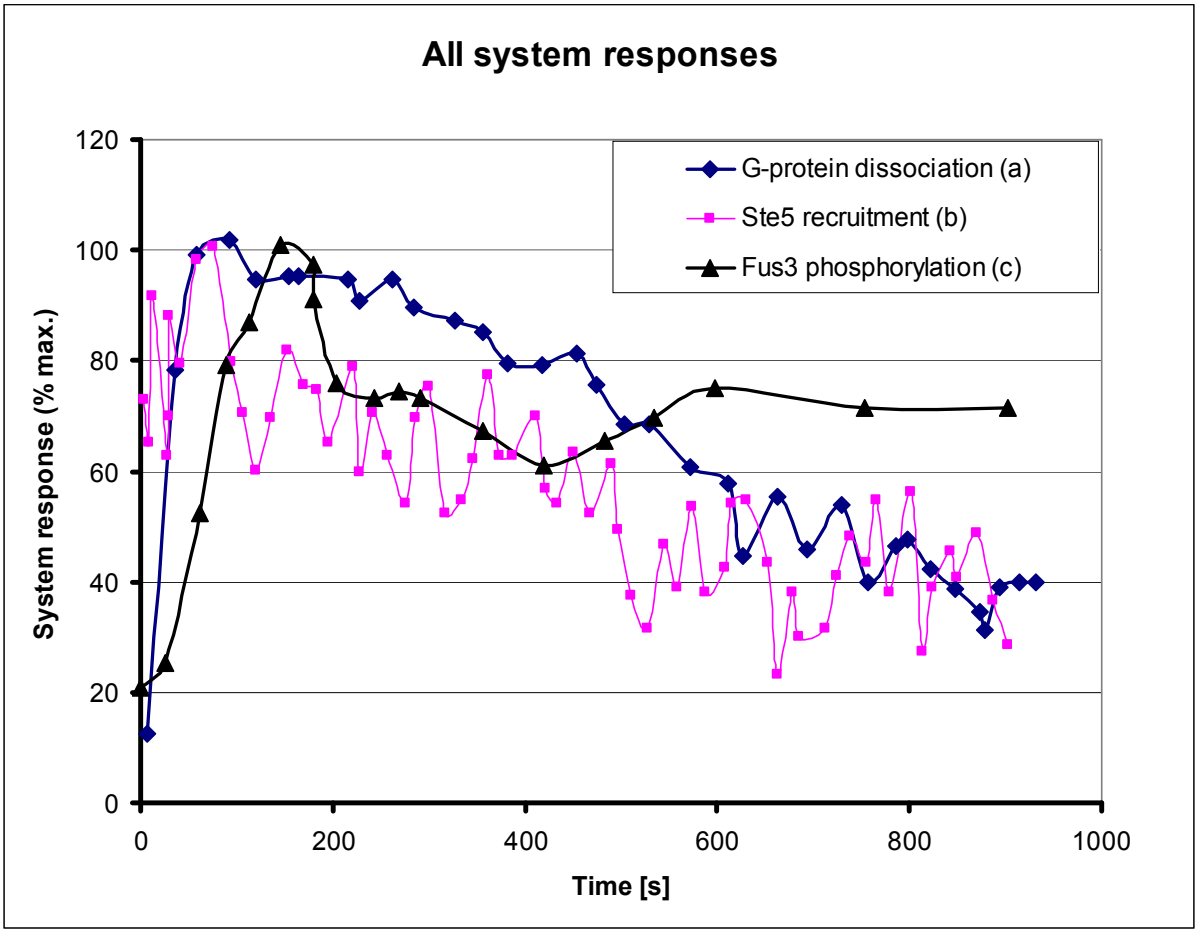

Figure 1.2: All system responses (a,b,c).
Data values are scaled to the corresponding maximum.

The signal that represents the dynamics of G-protein dissociation (Figure 1.2a) peaks rapidly in the first minute and declined to the plateau. The dynamics of

Ste5 (Figure 1.2b) membrane recruitment seems to be nearly similar to the dynamics of G-protein dissociation: the signal peaks rapidly in the first minute and decline to a plateau. The level of phosphorylated Fus3 (Figure 1.2c) increases quickly within the first 2 minutes and declines to a plateau after reaching the maximal value, forming a "Fus3-overshoot".

All measurements represent a similar signal dynamics after pheromone stimulation: "peak and decline". This fact indicates a possible existence of a negative feedback that may be also responsible for existence of the dose-response alignment [Yu *et al.* 2008].

1.5 Dose-response alignment

In wild type cells, the dose-response curves of receptor occupancy and pathway output align closely (Figure 1.3). The dose-response alignment (Figure 1.4) can be defined as proportional relationship (proportionality constant k≈1) between receptor occupancy and downstream system response, for example the amount of phospohorylated Fus3.

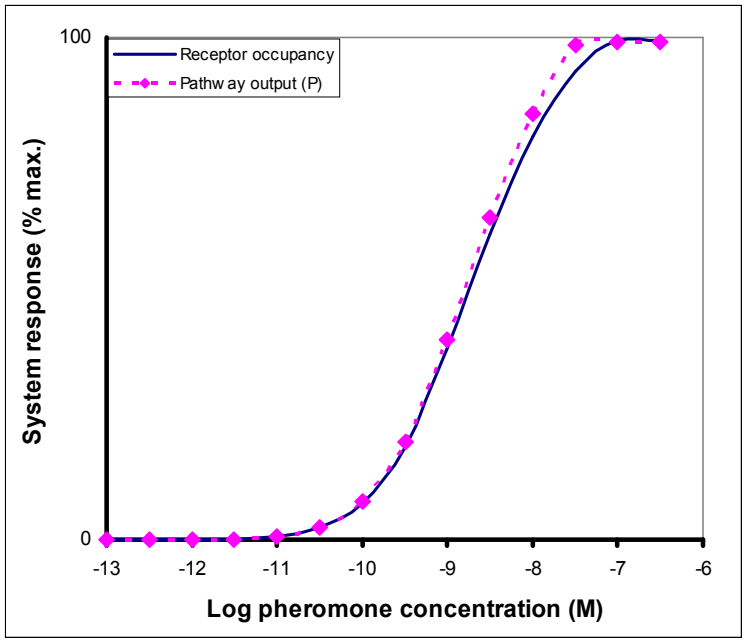

Figure 1.3: Dose responses of receptor occupancy and pathway output align closely

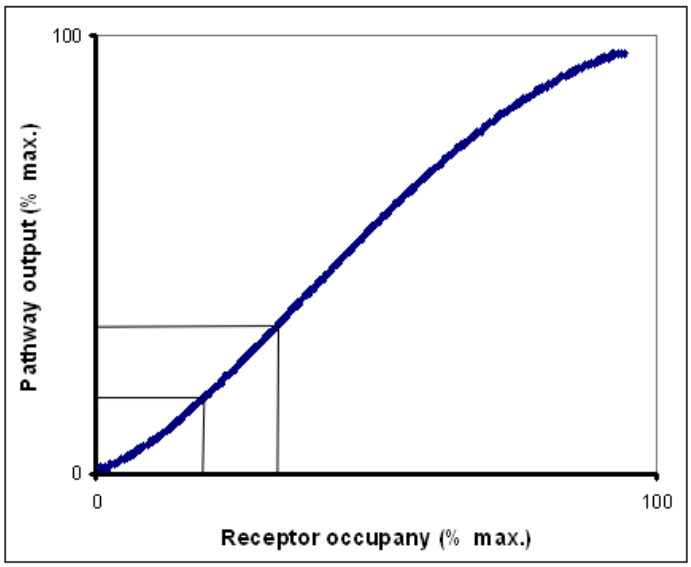

Figure 1.4: Dose-response alignment

In case of dose-response alignment changes in receptor occupancy correspond to the changes in pathway output that improves the fidelity of information transmission [Yu *et al*. 2008].

In a case when the pathway output is more sensitive than in the wild type, the dose-responses curves do not align closely anymore (Figure 1.5). The proportional relationship disappears (Figure 1.6).

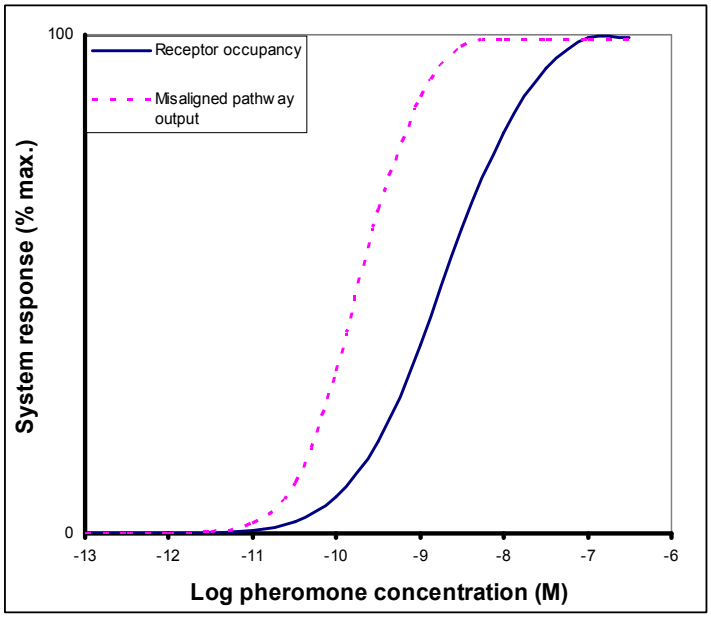

Figure 1.5: Dose responses of receptor occupancy and pathway output do not align

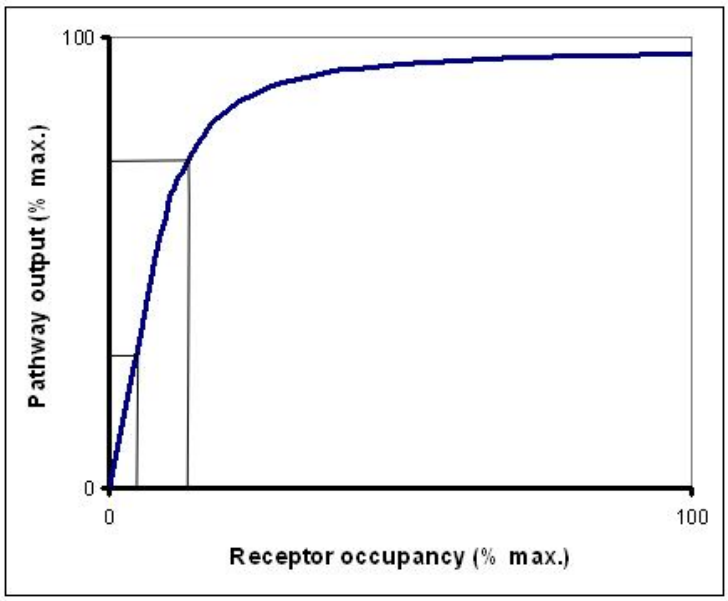

Figure 1.6: Dose-response misalignment

By misalignment even a slight noise in the receptor occupancy can result in a destruction of the fidelity of information transmission.

2 Theoretical background & methods

2.1 Mathematical modelling of reaction networks with ODE systems.

One of the most common methods to describe the rates of temporal concentration changes in a biological reaction system is the use of a set of ordinary differential equations (ODEs). In a system with n metabolites with concentration c_i (i=1,2,…, n), m reactions with rates v_j (j=1,2,…m) and stoichiometric coefficients n_{ij}, the dynamics of concentrations changes can be described by the following equations [Kofahl & Klipp 2006]:

$$\frac{dc_1}{dt} = f_1(c_1, c_2, ..., c_n) = n_{11} \cdot v_1 + n_{12} \cdot v_2 + ... + n_{1m} \cdot v_m$$
$$\frac{dc_2}{dt} = f_2(c_1, c_2, ..., c_n) = n_{21} \cdot v_1 + n_{22} \cdot v_2 + ... + n_{2m} \cdot v_m$$
M
$$\frac{dc_n}{dt} = f_n(c_1, c_2, ..., c_n) = n_{n1} \cdot v_1 + n_{n2} \cdot v_2 + ... + n_{nm} \cdot v_m$$

what is equivalent to:

$$\frac{dc_i}{dt} = \sum_{j=1}^{m} n_{ij} \cdot v_j \ .$$

The rate of a reaction can depend on the concentration of substrates, products and modifiers. All forms of a protein (unbound, complex forms, phosporylated and unphosphorylated) are treated as individual species in the model. All complex formations and dissociations as well as activations and deactivations can be defined as reactions with corresponding rates.

Initial concentrations of the species are obtained from the literature (if possible). All parameters are determined by fitting of the model to the experimental data.

The simulation of the dynamics of the models has been created with the software COPASI (Hoops, S., Sahle, S., Gauges, R., Lee, C., Pahle, J., Simus, N., Singhal, M., Xu, L., Mendes, P., and Kummer, U., 2006). The ODEs were solved by the LSODA method. LSODA (Petzold L. and Hindmarsh A., 1983) solves ODEs using stiff and non-stiff methods, begins with the non-stiff method and dynamically monitors data in order to optimize the results.

2.2 Parameter estimation

The goal of parameter estimation is to find a particular set of parameters in order to fit simulated data curves to the given experimental data with the most accuracy. There are given n experimental data points (x_i, y_i) and fitted data points (x_i, $f(x_1)$) with:

$$f(x_i) = \hat{y}_i$$

and

$$\varepsilon_i = \hat{y}_i - y_i .$$

The fitting function describes the data with the best accuracy when the value of RSS (sum of squared residuals) is minimized.

$$RSS = \sum_i^n \varepsilon_i^2 = \sum_i^n (\hat{y}_i - y_i)^2 \rightarrow \min$$

All parameters in this thesis were estimated with the method Evolutionary Programming. This technique mimics evolution and is based on two main rules: reproduction and selection [Hoops *et al.* 2006]. The Evolutionary programming algorithm contains a number of individuals that reproduce and compete. They reproduce asexually by creating a copy of itself exactly the same as the parent. During this process the child undergoes a slight mutation. Each of the individuals is a possible solution of the estimation and can be described in a form of a "genome". The genome consists of genes that correspond to the searched parameters. At the end of the generation, the number of individuals has doubled. Then all of the individuals are compared and ranked. The individuals with the

worse fitness (quantification of the optimality of the fit) are eliminated and so the population size is reduced.

There are three parameter options which values have to be chosen in order to use this method:

- Number of generations – for the time course simulations of the model a value from the range [200, 600] has been set;
- Population size – number of individuals at the beginning and the number of individuals that survive after the end of each generation as well. For the model, the population size was set from the range [20,40]:
- Seed- parameter that contains the information for the random number generator. The chosen value is 0 and is interpreted by COPASI as instruction to select always a random value.

2.3 Model selection and Akaike's Information Criterion (AIC)

The selection of a suitable model among many considered models is a basic problem in statistical modelling. Especially for models containing many parameters it is difficult to find the one that fits well the data and is not overparameterized. To find the best approximating model that represents a given data set among many competing models containing different number of parameters a simple criterion is needed [Bozdogan 1987]. The Akaike's Information Criterion (AIC) is an entropy-based information criterion developed by Hirotsugu Akaike in 1971 and can be calculated with the following formula:

$$AIC = 2k + n[\ln(RSS / n)],$$

where:

$$RSS = \sum_{i=1}^{n} \hat{\varepsilon}_i^2 \quad .$$

Here:

- RSS is the residual sum of squares of the fitted model;

- n is the number of observations;
- k is the number of parameters.

The AIC takes into account two attributes: the accuracy of measurement and the complexity of the model. The best model should have the least possible complexity as well as contain the most information about the data. A single value of AIC is useless unless it is compared with computed values for all considered models [Burnahm 2004]. The model with the smallest AIC value over all models is the best approximating model.

2.4 Parameter Sensitivity Analysis

Parameter sensitivity analysis is used to find out how the perturbations of the input parameters determine the changes in the output of the model [Kamrunnahar *et al.* 2004]. This analysis is helpful in searching for the parameters that have the most impact on the output of the system. The sensitivity is defined as the change in output (ΔO) to the change in the parameter (ΔP) value normalized with the factor P/O that makes it independent of the units and of the magnitude of P and O [Klipp *et al.* 2005]:

$$S = \frac{\Delta O}{\Delta P} \cdot \frac{P}{O}.$$

To calculate the sensitivity values the tool COPASI was used. As the subtask method Time series was set, as function Non-Constant Concentrations of Species was chosen and as values all parameters were set.

COPASI calculate sensitivities using a slight different formula:

$$S_{COPASI} = \frac{\partial O}{\partial P}.$$

COPASI uses numerical differentiation with finite differences to calculate the sensitivities of the model.

There are two parameter options for the sensitivities calculation:

- Delta factor – multiplied with an absolute value of the concentration of the species return the value of delta. If it is smaller than delta minimum, the value of delta minimum is used instead. As delta factor a default value of 10^{-6} has been set.
- Delta minimum - represent the minimal delta, has been set to 10^{-12}.

3 Data

3.1 Data plots

The data used for the parameter estimation were provided by Richard Yu from The Molecular Science Institute, Berkley, USA, published as well as discussed in [Yu *et al.* 2008].

Data values are scaled to the peak signal value in cells which where simulated only with pheromone.

Indications:

- P - cells stimulated with 100nM pheromone;
- P+I – cells stimulated with 100 nM pheromone and 10 μM 1-NM-PPI (4-amino-1-(tetr-butyl)-3-(1'-naphthylmethyl)-pyrazolo[3,4-d] pyramidine) – inhibitor;
- U – untreated cells.

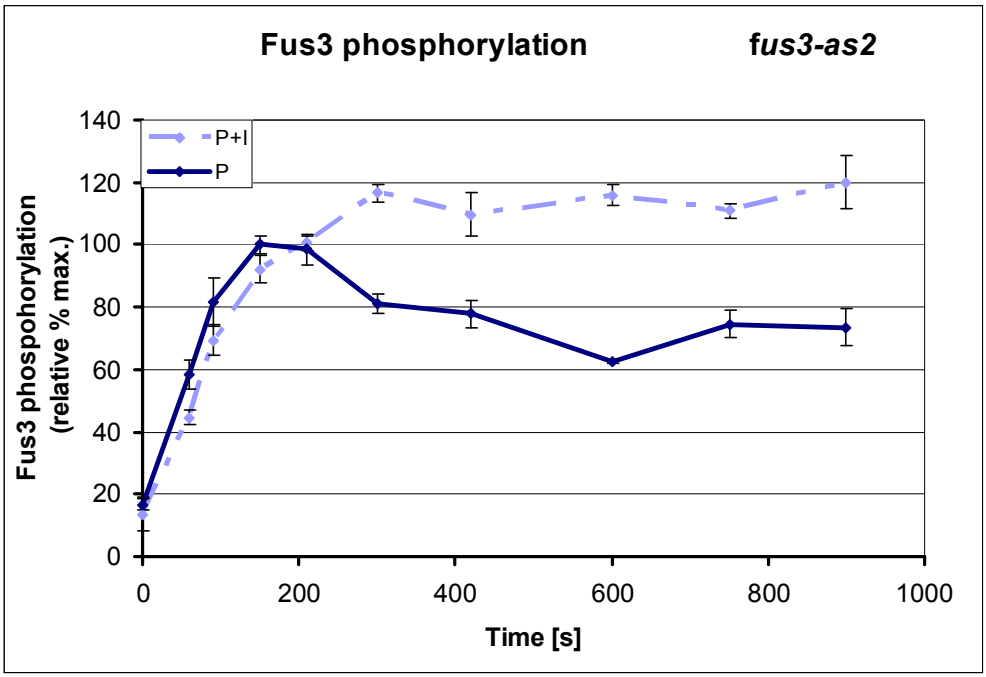

Figure 3.1: Fus3 phosphorylation (fus3-as2)

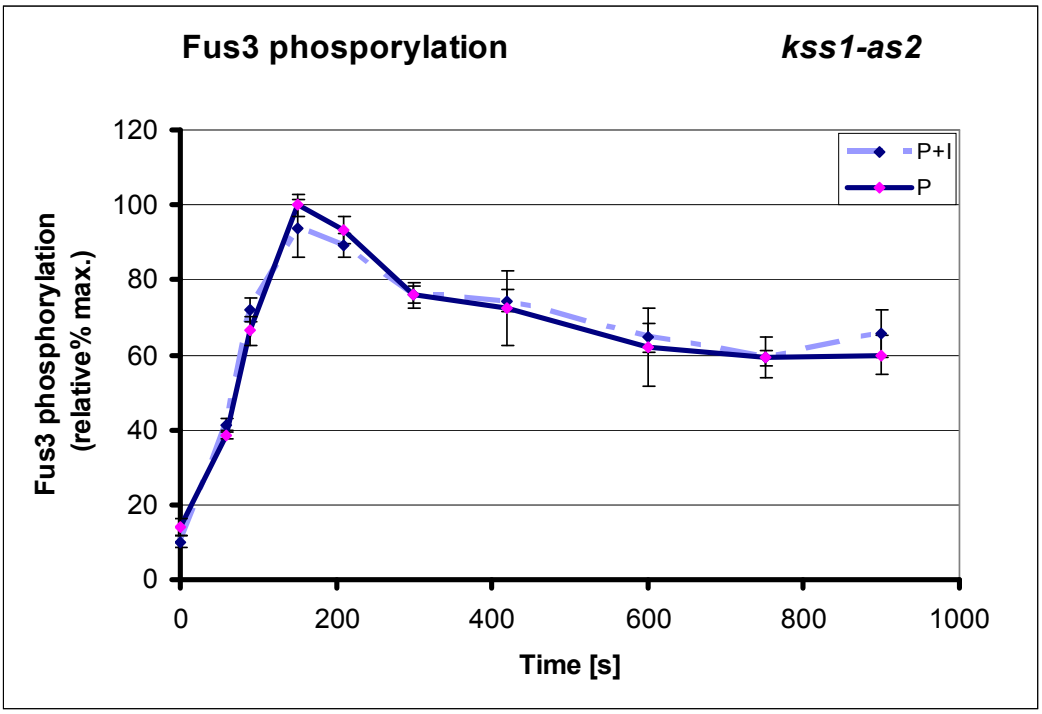

Figure 3.2: Fus3 phosphorylation (kss1-as2)

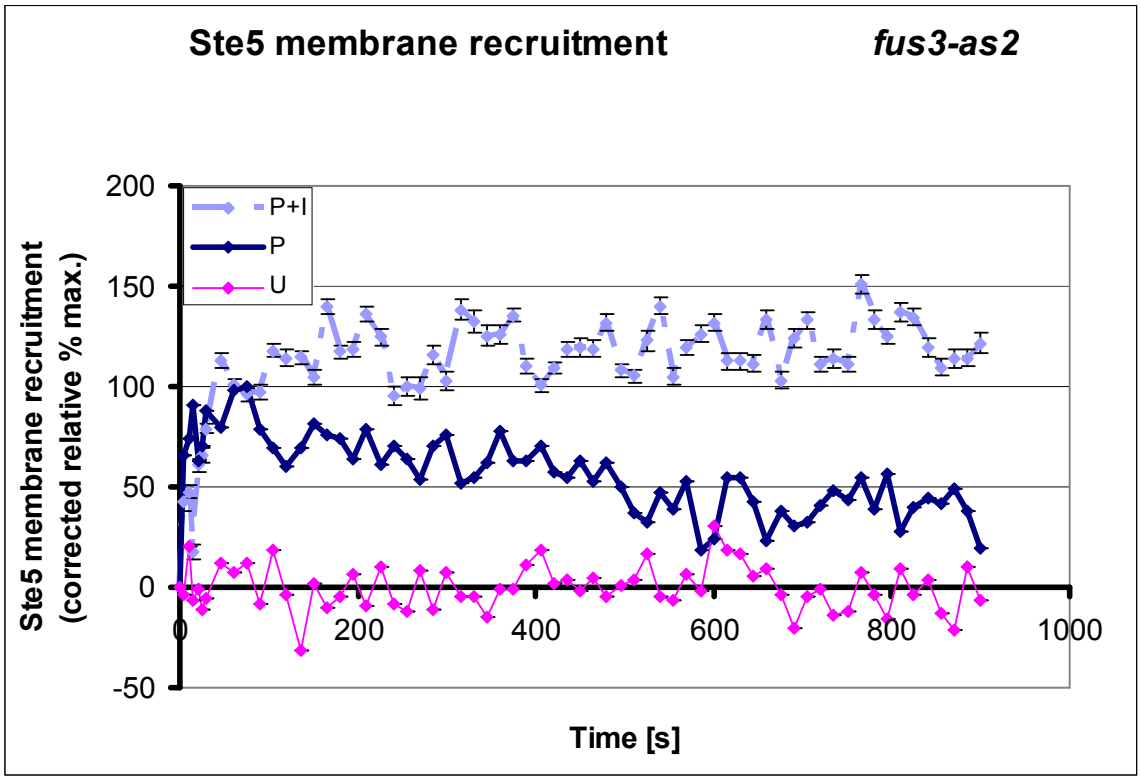

Figure 3.3: Ste5 membrane recruitment (fus3-as2)

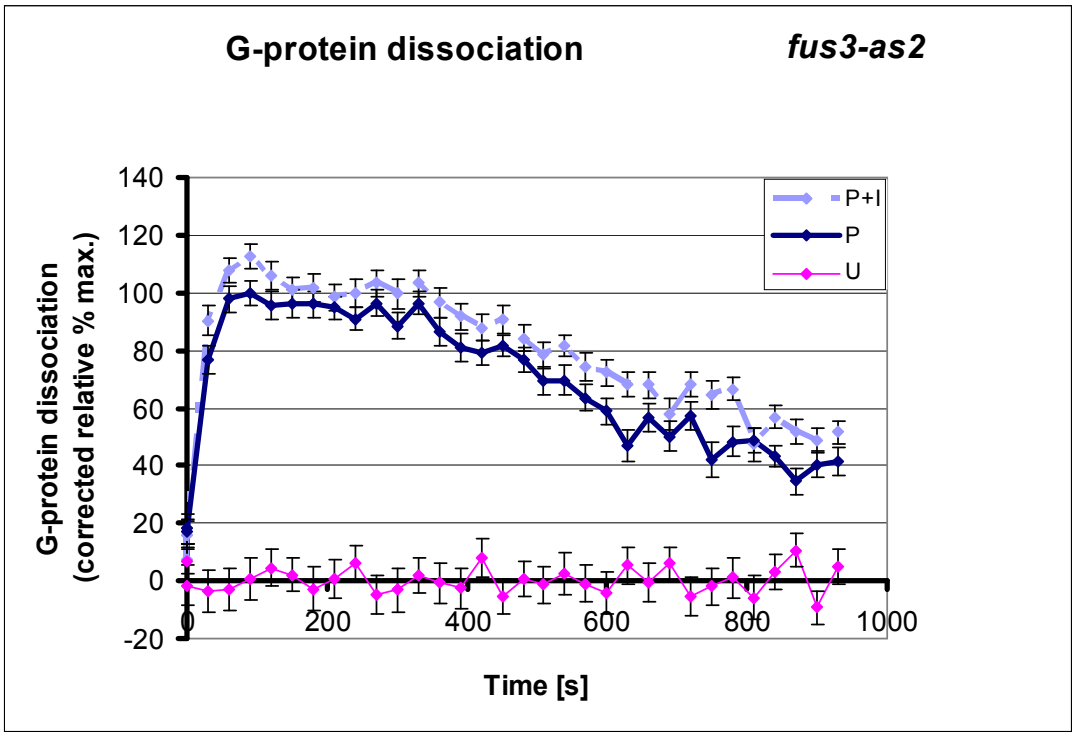

Figure 3.4: G-protein dissociation (fus3-as2)

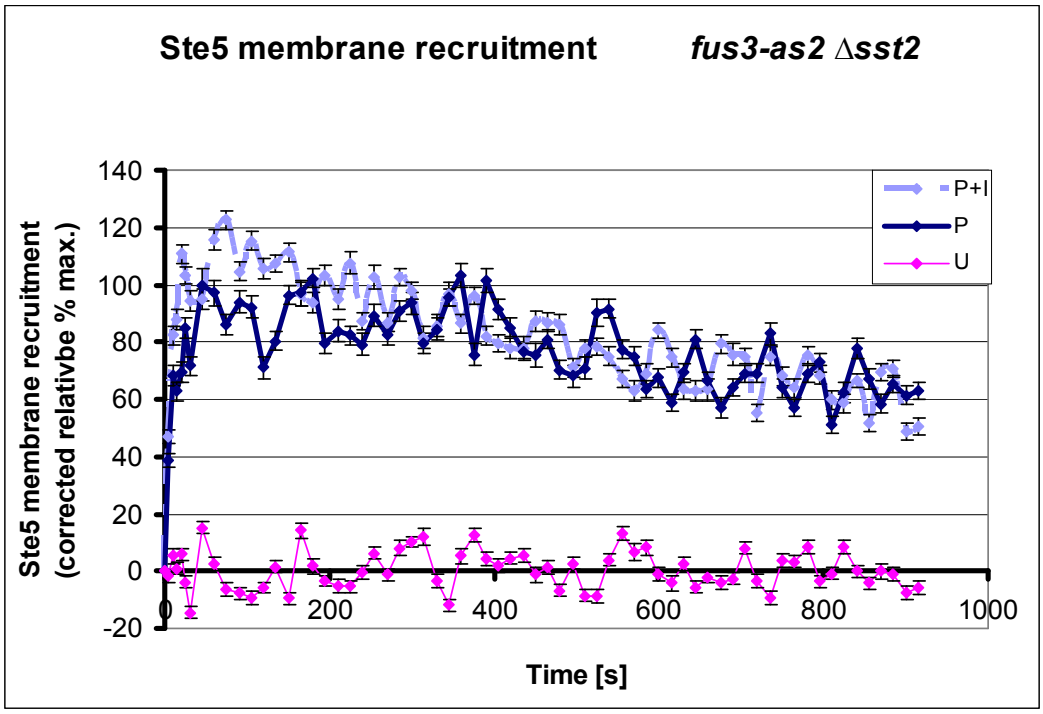

Figure 3.5: Ste5 membrane recruitment (fus3-as2 Δsst2)

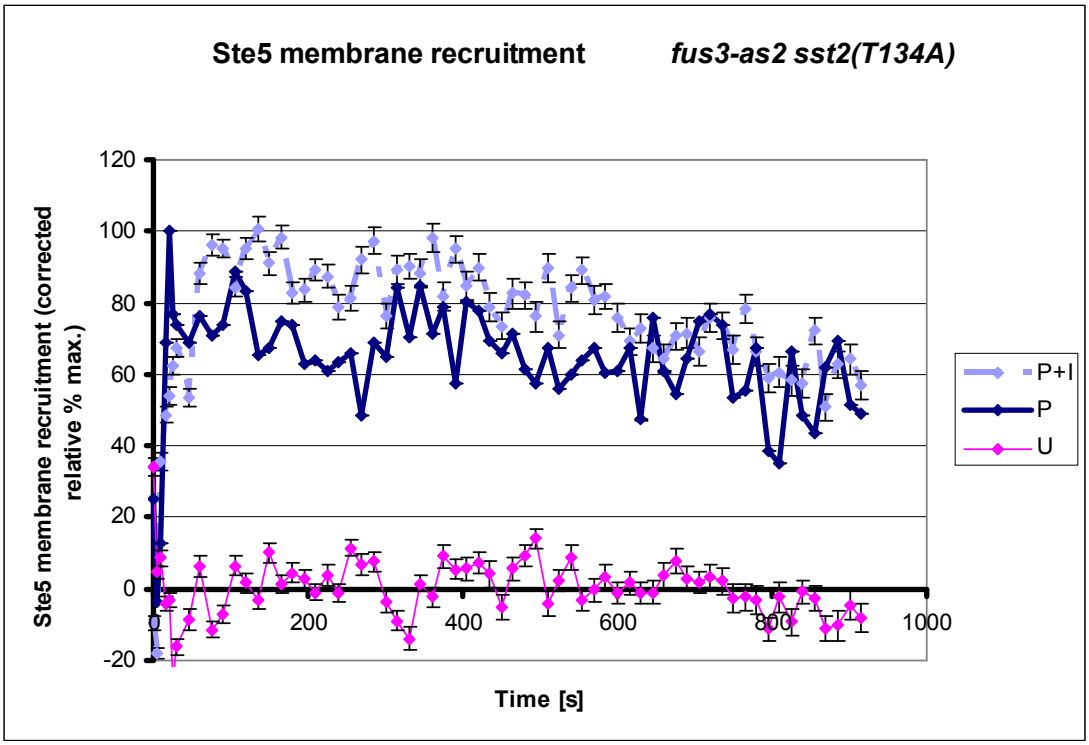

Figure 3.6: Ste5 membrane recruitment (fus3-as2 sst2 T134A)

Diverse techniques were used to follow the dynamics of these processes. To measure the G-protein dissociation the loss of fluorescence resonance energy transfer FRET between Gα subunit and protein Ste18 was measured. The Ste5 membrane recruitment was quantified by measuring the transfer of yellow fluorescent protein (YFP) tagged Ste5 from the nucleus and cytosol to the membrane. The dynamics of Fus3 phoshorylation was measured using quantitative immunoblotting.

3.2 Discussion of the data

Many previous references have already suggested the existence of a negative feedback in the pheromone signalling cascade in yeast [Shao *et al.* 2006, Colman-Lerner *et al.* 2005]. The presented data give not only a clear answer to the question which of the MAPKs, Fus3 or Kss1 mediate this feedback, but also explain partially the mechanism of this regulation. Figures 3.1 and 3.2 compare the levels of Fus3 phosphorylation in two mutant cells: fus3-as2 and kss1-as2. The cells fus3-

as2 and kss1-as2 contain mutant kinases that are active during the pheromone (P) stimulation, but their activity is inhibited during the pheromone + inhibitor (P+I) stimulation. As a result, the Fus3 phosporylation level in fus3-as2 cells does not decline to a plateau during the inhibition, but remains nearly constant after reaching the peak (Figure 3.1). There is no change in the dynamics of Fus3 phosporylation in the kss1-as2 cells (Figure 3.2) that indicates that the MAPK Fus3 is involved in the mechanism of the negative feedback in the system [Yu *et al.* 2008].

The next problem to solve was to identify the place, where the Fus3 mediated feedback acts. The dynamics of two processes was considered: G-protein dissociation and Ste5 recruitment. The inhibition of Fus3 kinase activity does not cause changes in the G-protein dissociation dynamics (Figure 3.4), but has a visible influence on the Ste5 membrane recruitment (Figure 3.3) and modifies the default dynamic of this process. It indicates that the Fus3-mediated feedback acts on or upstream of Ste5 recruitment to the membrane and downstream of G-protein dissociation.

In order to explain the mechanism of the Fus3-mediated negative feedback, the Ste5 membrane recruitment was measured in cells without Sst2. After deleting Sst2, the inhibition of Fus3 kinase activity has no effect on the dynamics of Ste5 membrane recruitment (Figure 3.5). In this case Ste5 recruitment (with and without the inhibitor) looks similar to one in the cells with Sst2, that were stimulated with pheromone. This finding confirms that the 'peak and decline' behaviour is the default behaviour in absence of Sst2. Taking this and previous findings into account, it is likely that Sst2 regulates positively the Ste5 membrane recruitment and that this regulation is negatively regulated by Fus3.

A different crucial finding for the understanding of the negative feedback mechanism is the fact that the dynamics of Ste5 membrane recruitment in mutant strain sst2(T134A) is similar to the dynamics in Δsst2 (Figure 3.5 & Figure 3.6). This fact allows to claim that the T134A (Fus3 phosphorylation site in DEP1

domain of Sst2) mutation responsible for the disruption of the positive feedback of Sst2 on Ste5 membrane recruitment.

4 Model construction

The aim of this work was to propose a molecular mechanism of the feedback that explains the experimental data satisfying. The task was to combine the previous knowledge about the mechanism of the pheromone pathway [e.g. Kofahl & Klipp 2004, Shao *et al.* 2006] with the new concepts [Yu *et al.* 2008]. More than 50 different variants of model had been tested that vary in complexity, number and kinds of feedback as well as in reaction kinetics. To give an overview, four of them had been chosen and are presented in detail.

The following part of the model structure (Figure 4.1) is common in all selected and discussed model structures (Model 0):

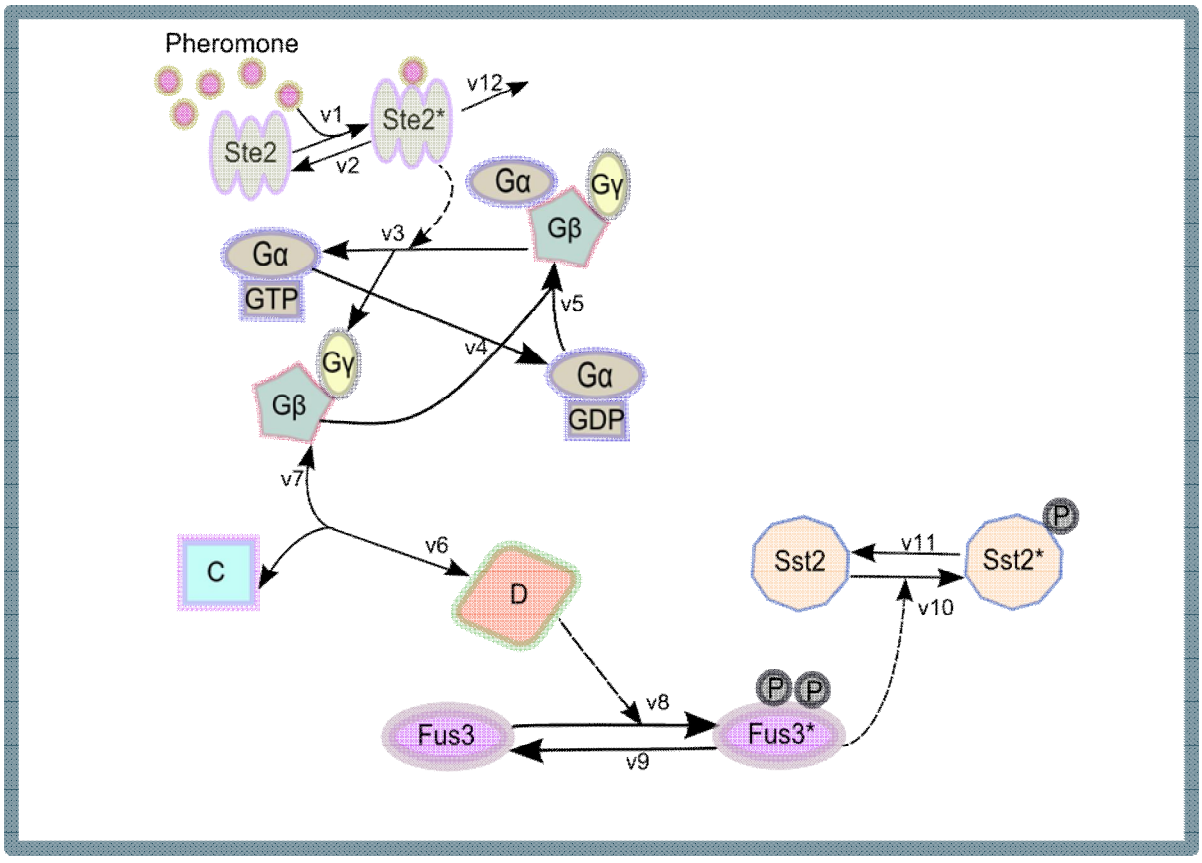

Figure 4.1: The common part of all model structures - Model 0

This structure, Model 0 (Figure 4.1) is a simplification and does not contain all species and modifiers. However, it still describes sufficiently the mechanism of the pheromone pathway. The receptor Ste2 is activated (v_1) in the presence of

pheromone. The activated receptor Ste2 causes the G-protein dissociation (v_3) into GαGTP and G$\beta\gamma$ or can be deactivated (v_2) as well as degraded (v_{12}). The G protein subunits can the reassociate (v_4, v_5) or the subunit G$\beta\gamma$ can bind (v_6) to the scaffold protein (C) building a complex (D) that activates the MAPK cascade that leads to the activation of Fus3 (v_8). Activated Fus3 may activate Sst2 by phosporylation (v_{10}), as well as be deactivated (v_9). Activated Sst2 may also be deactivated (v_{11}) that is a constitutive step for the mechanism.

In the chosen model structures, the repetitive components are supplemented with different feedbacks as well as delays.

4.1 Model A

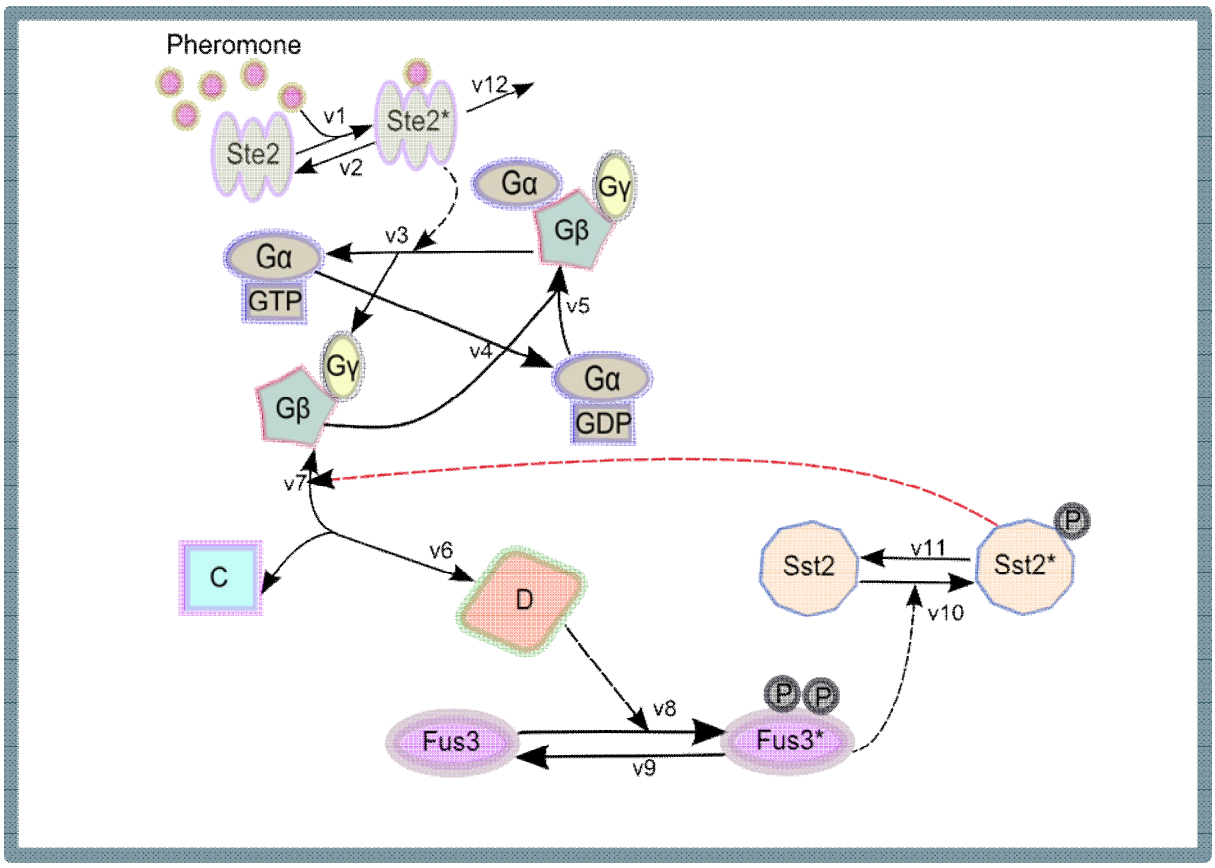

Figure 4.2: The structure of Model A

In case of Model A (Figure 4.2), Model 0 is supplemented with an extra feedback mediated by Sst2* that promotes the dissociation of complex D into G$\beta\gamma$ and the scaffold complex and therefore can be interpreted as a negative feedback of Fus3* on scaffold protein recruitment.

4.2 Model B

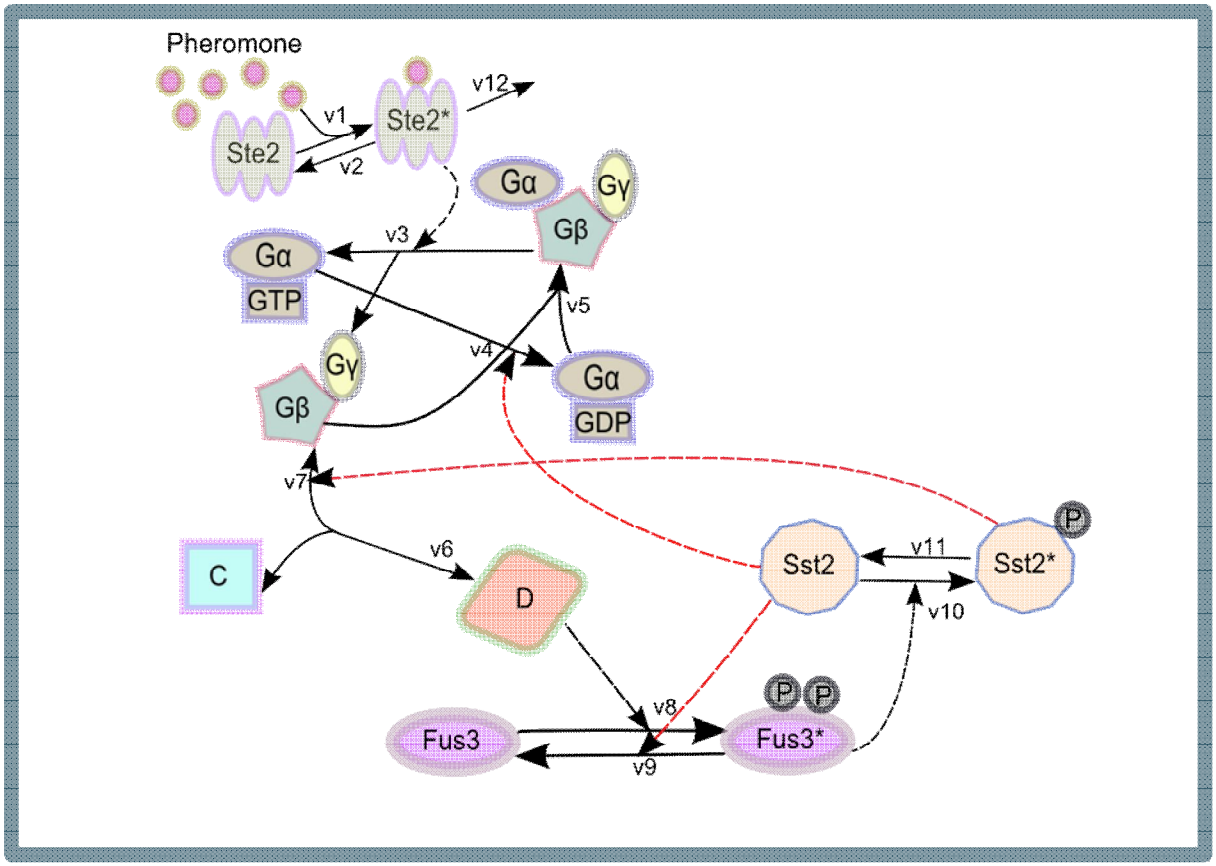

Figure 4.3: The structure of Model B

The difference between Model 0 and Model B (Figure 4.3) is the existence of 3 feedbacks. One of them is mediated by Sst2* (as in Model A) and other two are mediated by Sst2. Although the experimental data suggest that there is no feedback on the reassociation of G-protein, an extra feedback of Sst2 promoting the reassociation is included in this model due to suggestions in previous models [e.g. Klipp & Kofahl 2004].

4.3 Model C

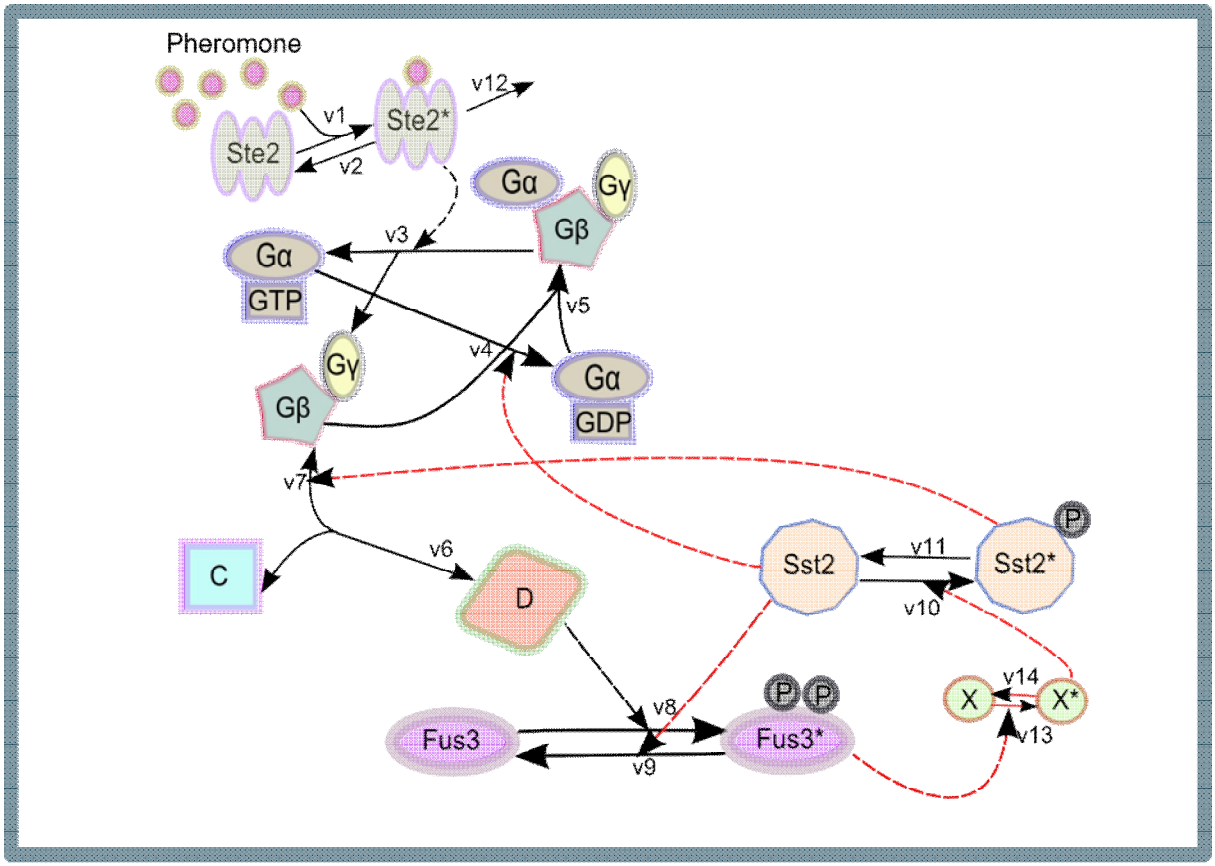

Figure 4.4: The structure of Model C

Model C (Figure 4.4) is based directly on Model B with one exception: there is an extra delay in activation of Sst2 by Fus3*. This additional step depends on activation and deactivation of a protein X where the activation is mediated by Fus3*. The activated form of X, X* activates then the Sst2.

4.4 Model D

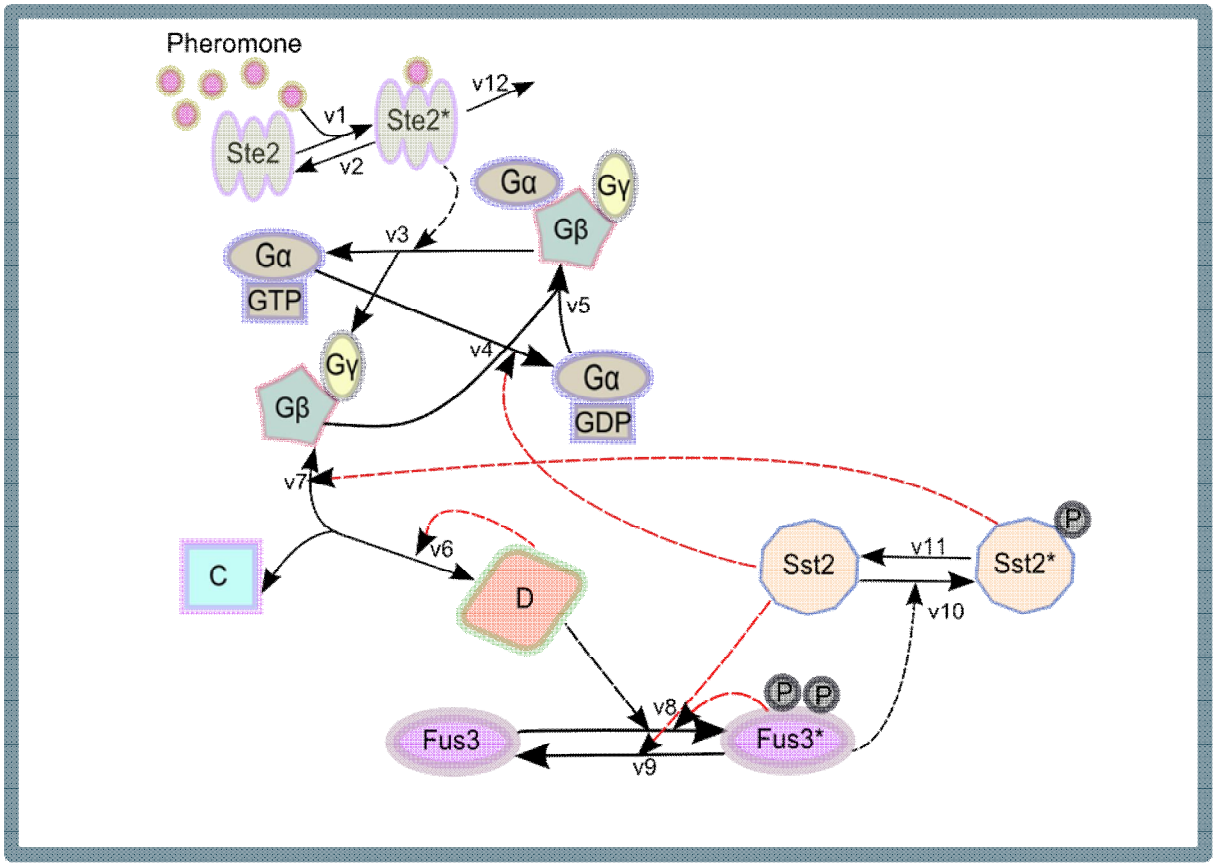

Figure 4.5: The structure of Model D

Model D (Figure 4.5) is also directly based on Model B with two additional autoregulation feedbacks. The Fus3* and the D positively mediate their own activation and production, respectively.

Values of initial concentrations of components as well as equations that describe the dynamics of the models can be found in the appendix.

5 Results

5.1 Results of parameter estimation

For each of chosen model structures parameters have been estimated with the tool COPASI (method described in 2.2). All estimations are based on 6 data sets (3 experiments in two options each, a total of 214 observations):

- Fus3 phosporylation in fus-as2 cells stimulated with only pheromone;
- Fus3 phosporylation in fus-as2 cells stimulated with pheromone and inhibitor;
- Ste5 membrane recruitment in fus-as2 cells stimulated with only pheromone;
- Ste5 membrane recruitment in fus-as2 cells stimulated with pheromone and inhibitor;
- G-protein dissociation in fus-as2 cells stimulated with only pheromone;
- G-protein dissociation in fus-as2 cells stimulated with pheromone and inhibitor.

The results are presented in form of graphs that show the experimental data with the corresponding fits. The fits are the results from the parameter estimation and represent the system response in each case. For the stimulation with both pheromone and inhibitor, the kinase activity of Fus3* has been blocked in the way that the constant k_{10} (reaction v_{10}) has been set to 0 while estimating. The behaviour of the system in first 15 minutes (900s) after pheromone stimulation was simulated.

The simulated values have been scaled in the way that the maximum value while stimulating with only pheromone corresponds to 50% of the initial concentration.

5.1.1 Model A

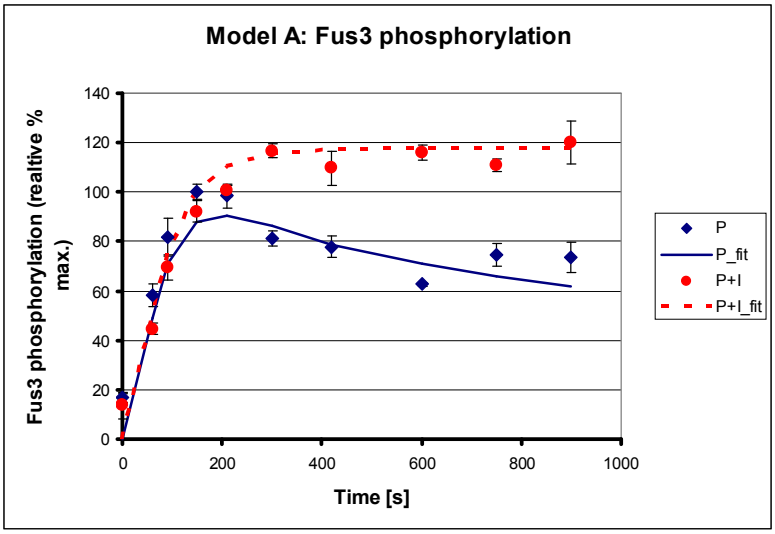

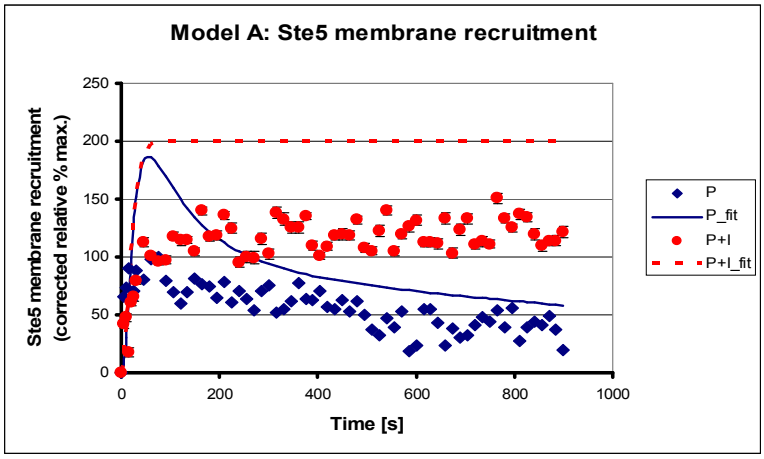

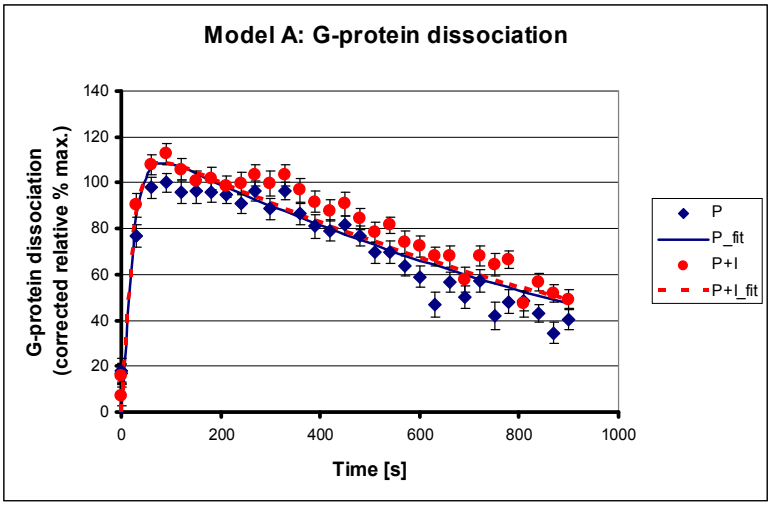

Figure 5.1: Results of parameter estimation: Model A

Data values are scaled to the peak signal measured during the stimulation with only pheromone. Indications: P - stimulation with only pheromone (experimental data); P+I - stimulated with pheromone and inhibitor (experimental data); P_fit -response of the model, stimulated with pheromone, P+I_fit – response of the model, stimulated with pheromone and inhibitor.

5.1.2 Model B

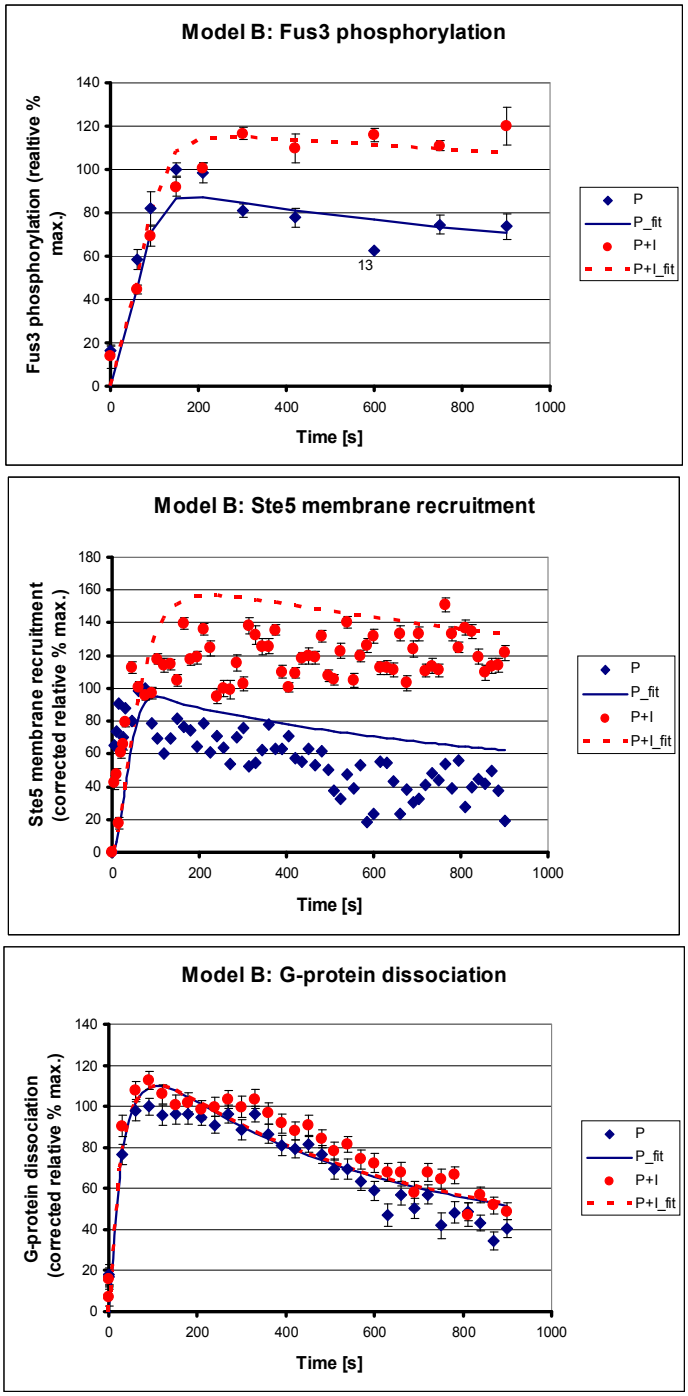

Figure 5.2: Results of parameter estimation: Model B

Data values are scaled to the peak signal measured during the stimulation with only pheromone. Indications: P - stimulation with only pheromone (experimental data); P+I - stimulated with pheromone and inhibitor (experimental data); P_fit -response of the model, stimulated with pheromone, P+I_fit – response of the model, stimulated with pheromone and inhibitor.

5.1.3 Model C

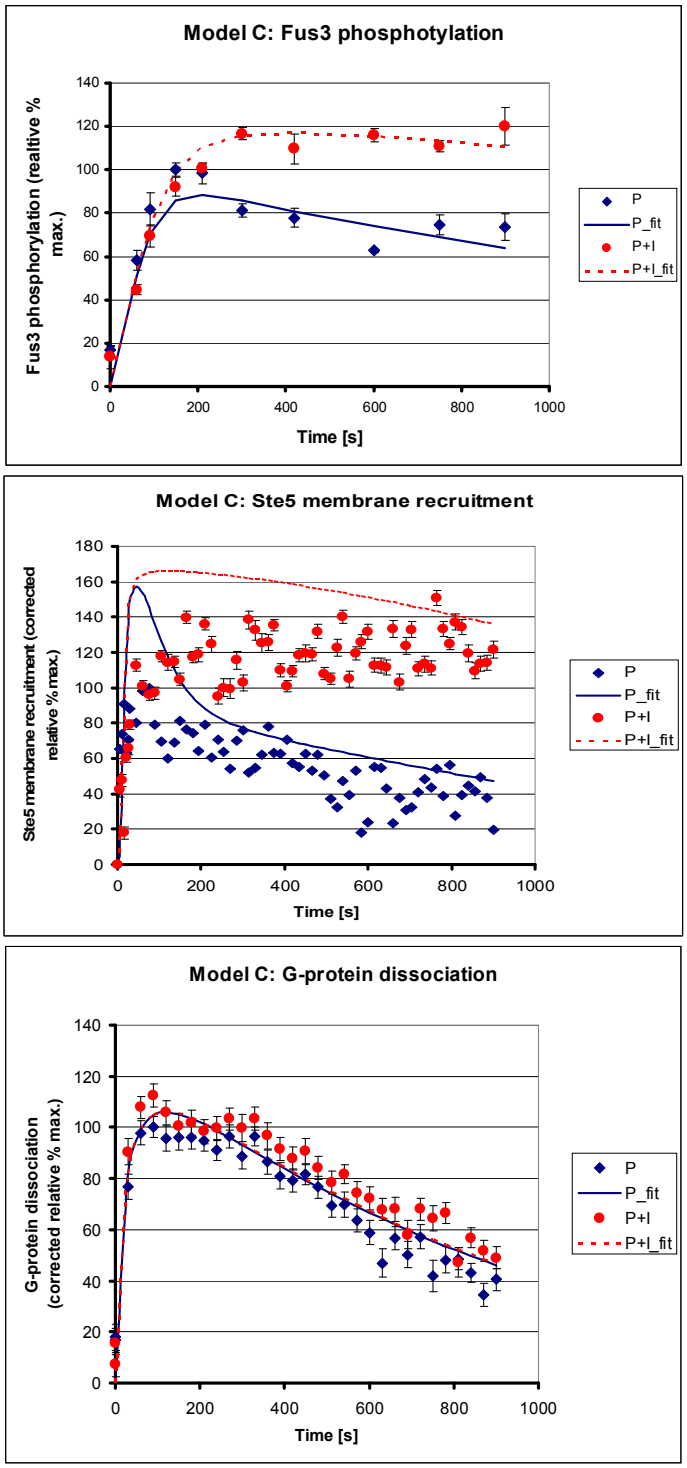

Figure 5.3: Results of parameter estimation: Model C

Data values are scaled to the peak signal measured during the stimulation with only pheromone. Indications: P - stimulation with only pheromone (experimental data); P+I - stimulated with pheromone and inhibitor (experimental data); P_fit -response of the model, stimulated with pheromone, P+I_fit – response of the model, stimulated with pheromone and inhibitor.

5.1.4 Model D

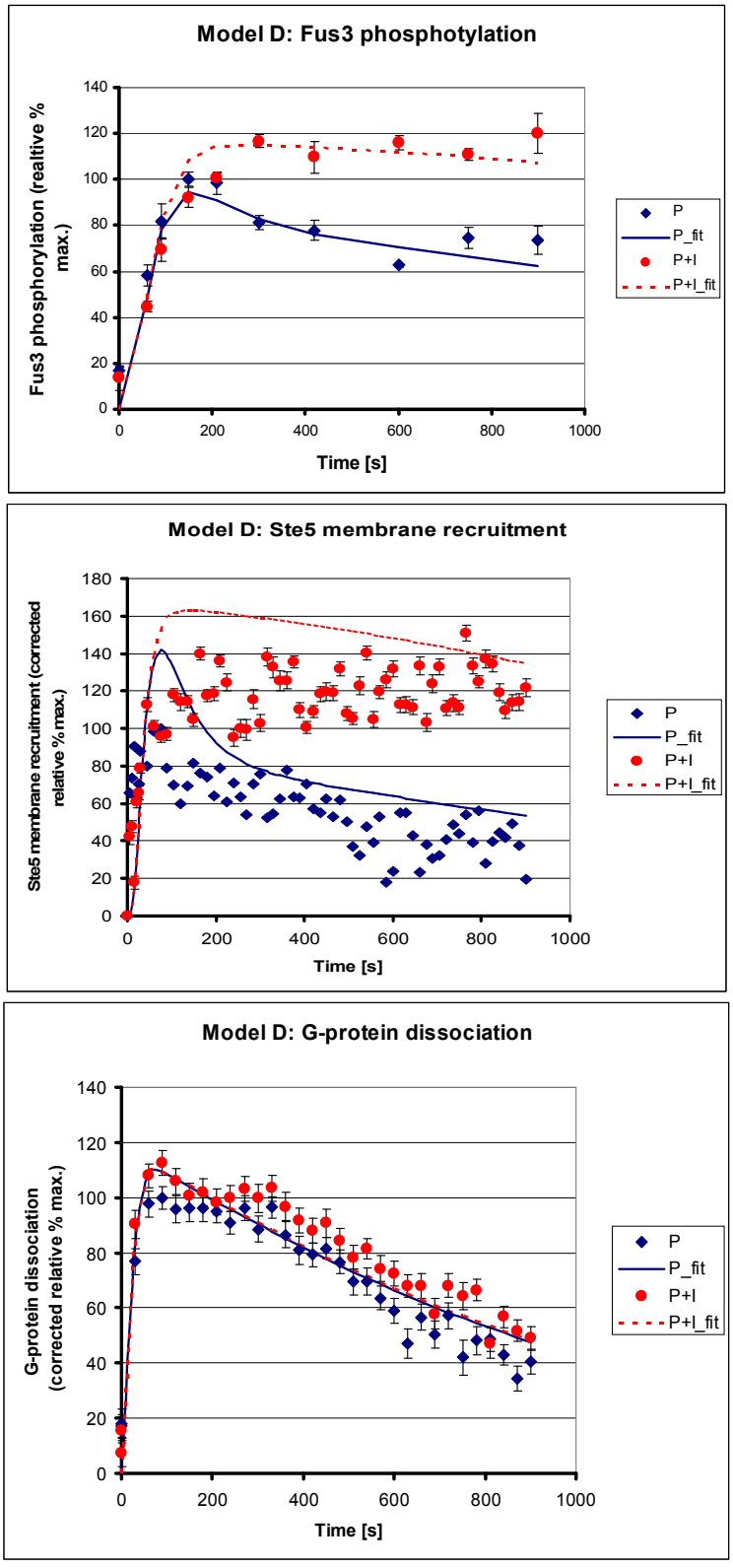

Figure 5.4: Results of parameter estimation: Model D

Data values are scaled to the peak signal measured during the stimulation with only pheromone. Indications: P - stimulation with only pheromone (experimental data); P+I - stimulated with pheromone and inhibitor (experimental data); P_fit -response of the model, stimulated with pheromone, P+I_fit – response of the model, stimulated with pheromone and inhibitor.

5.1.5 Results of parameter estimation – summary

Unfortunately, none of the model variants is able to produce such a response that perfectly reproduces all experimental data that have been taken into consideration. However, the results are still acceptable and can be evaluated.

The dynamics of Fus3 phosporylation with and without an inhibitor is described with the best fitness in model D. However, the fits in other models also relatively accurate.

The results of parameter estimation for Ste5 membrane recruitment are rather unsatisfying in all models. Although the requested behaviour "*peak and decline*" while stimulating with only pheromone and a "*constant after reaching a peak*" behaviour while stimulating with pheromone and inhibitor can be observed, there is no consistency in the peak value. In all models, the system dynamics reach a higher maximal value of recruited Ste5 to the membrane than in the reality. The experimental data are fitted best in model B, then in model C and model D.

All models well represent the data for the G-protein dissociation.

These results give no clear answer which of the models is the best model. The only conclusion that can be drawn from these results is the refusal of model A as a possible best model.

All values of estimated parameters can be found in the appendix.

5.2 Model selection

In order to find the most plausible model the values of AIC have been calculated and ranked. The number of observations has the same value (214) in all model options.

Model	RSS (objective value)	k (number of parameters)	AIC
B	123590,4	15	1390,77296
D	144799,3	17	1428,6654
C	176817,0	15	1467,41542
A	533690,1	13	1699,82126

Table 5.1: The calculated values of AIC

The minimal value of AIC has been calculated for model B. However, AIC values for model D and model C are not importantly higher (2,7% in case of model D and 5,5% in model C). The AIC value for model A is more than 22% higher that the AIC value for model B. These results supplement the results of parameter estimation with the conclusion that model B describes the dynamics of the processes with the most accuracy.

5.3 Predictions of the model: dose -response alignment

It was revealed that the negative feedback mediated by Fus3* is responsible for the dose-response alignment in the pheromone pathway, a proportional relationship between receptor occupancy and downstream response [Yu *et al.* 2008]. The altering pheromone concentration has been used as a simplified quantitative description of receptor occupancy. There are many alternative definitions of the downstream response. Here, the concentration of phosporylated Fus3 after 900 s has been used. The tool Mathematica (ver. 6.0) has been applied to calculate the final concentration of Fus3* for different pheromone concentrations

for all models. Both variants, with Fus3 not inhibited and inhibited, have been taken into consideration and additionally a sigmoid fit has been calculated.

All fitted curves are described with the following formula (Hill function):

$$\frac{a \cdot S^h}{K^h + S^h},$$

where S is the substrate (here the pheromone concentration) and a, K, h are constants.

To compare the results for all models the values of EC_{50} (the concentration required for a half-maximum response) for both Fus3 not inhibited and not inhibited have been calculated. Afterwards, it has been calculated how much the Fus3 inhibition reduces the EC_{50} value for each model.

Model	Reduction of EC_{50}
C	10,1-fold
A	7,5-fold
B	2,2-fold
D	2,2-fold

Table 5.2: Calculated values of reduction of EC_{50}.

The experimental data suggest that Fus3 inhibition reduces the EC_{50} value by ca. 20-fold. None of the model results in such a reduction, but the highest value has been calculated for model C. The predictions (predicted data points with corresponding Hill-fits) of model B, which has been chosen as the best model, and model C, which has the highest value of reduction of EC_{50}, are presented and compared. There is well-defined shift between the curves in model C (Figure 5.6) and a weak, but still recognizable shift between the curves in model B (Figure 5.5). The existence of the shift between the curves indicates that the inhibiton of Fus3 activity disrupts the dose responce alignment.

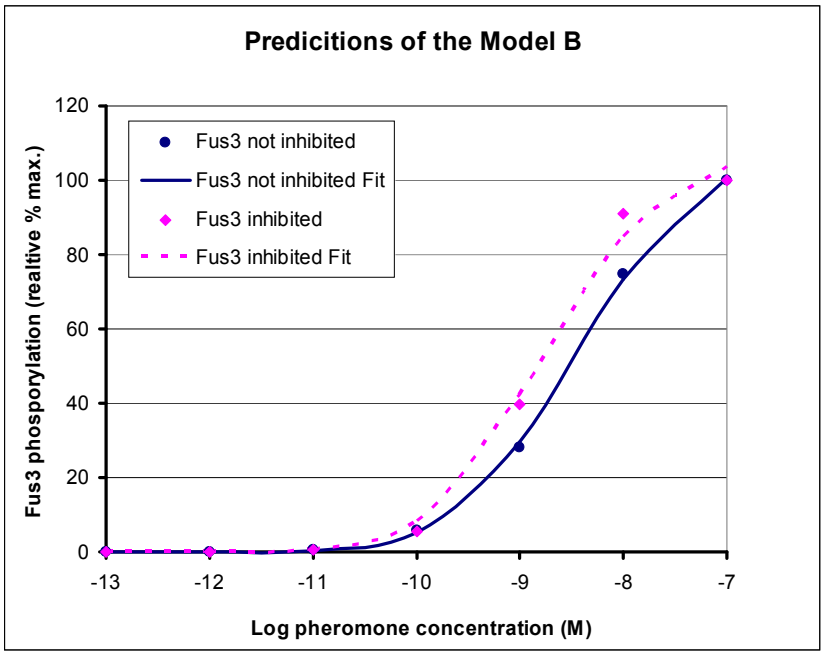

Figure 5.5: Model B: the disruption of the dose-response alignment
Data values are scaled to the maximal value.

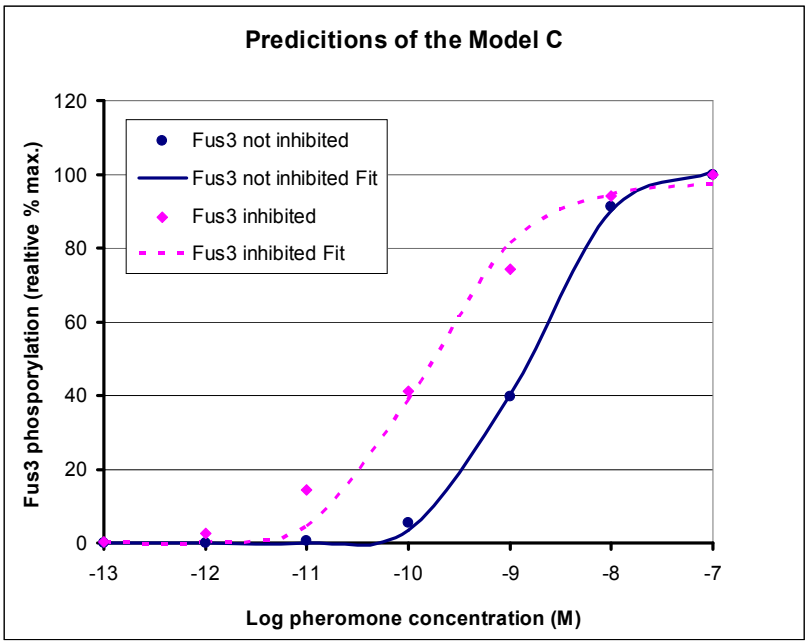

Figure 5.6: Model C: the disruption of the dose-response alignment
Data values are scaled to the maximal value.

Next, the fitted Hill functions that represent the predictions of the model have been compared with the experimental values from [Yu *et al.* 2008]. In order to find out which model predicts the experimental data with the most accuracy, the correlation coefficients has been calculated and compared.

	Correlation coefficients	
Model	Fus3 not inhibited	Fus3 inhibited
A	0,97	0,79
B	0,96	0,78
C	0,98	0,95
D	0,96	0,79

Table 5.3: Calculated values of correlation coefficients.

The correlation coefficients of model C have the highest value and therefore the predictions of model C reproduce the experimental data best. Figure 5.7 & 5.8 compare of the predictions of model B and model C with the experimental data.

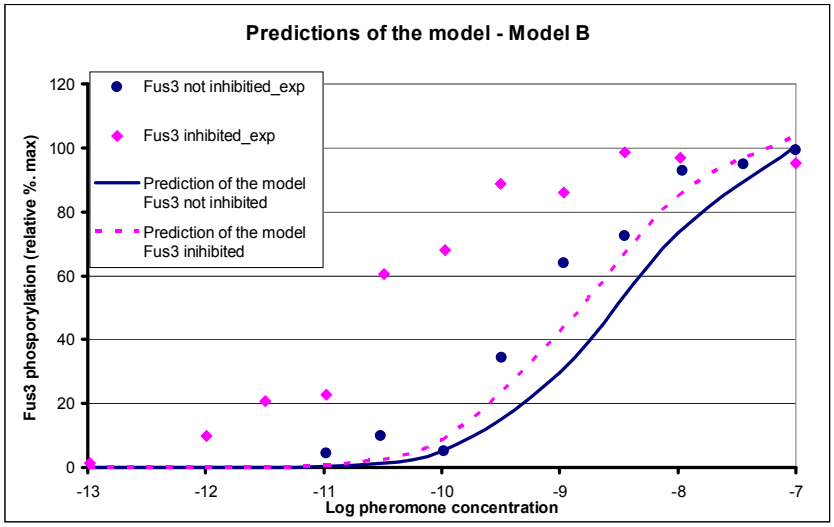

Figure 5.7: Predictions of the Model B compared with experimental data
Data values are scaled to the maximal value

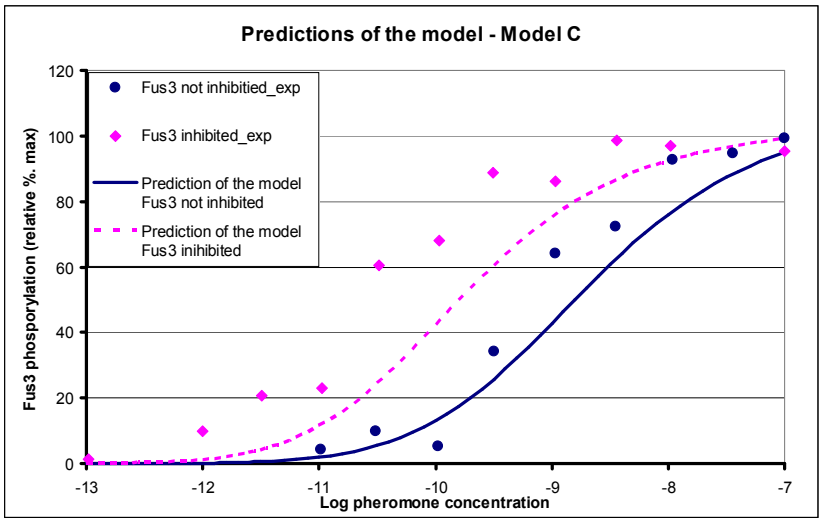

Figure 5.8: Predictions of the Model C compared with experimental data
Data values are scaled to the maximal value.

The predictions of model C are significantly better than the predictions of model B. However, these predictions only consider the final concentrations of Fus3 after 900 seconds. The changes in the dynamics of Fus3 phosphorylation depending on the change in pheromone concentration have been disregarded and not discussed.

5.4 Parameter sensitivity analysis

In order to find out how much the concentration of the output (Fus3* after 900s) changes when a particular kinetic parameter varies, the values of sensitivities have been calculated for all models and discussed for models B and model C. The values of the sensitivities reveal also which of the parameter have the biggest impact on the concentration of the output.

Calculated sensitivities:

Parameter	[Fus3*][900]	
	Model B	Model C
k_1	-0,018	-0,031
k_2	0,012	-0,00001
k_3	0,084	0,237
k_4	-0,00003	-0,085
k_{41}	0,00033	0,004
k_5	-0,194	-0,131
k_6	0,334	0,444
k_{61}	---	---
k_7	-0,079	-0,049
k_{71}	-0,262	0,367
k_8	0,495	0,601
k_{81}	---	---
k_9	-0,0000007	0,001
k_{91}	-0,502	-0,651
k_{10}	-0,232	-0,357
k_{11}	0,232	0,373
k_{12}	-0,100	-0,400
k_{13}	---	-0,357
k_{14}	---	0,373

Table 5.4: Calculated sensitivities

Positive (negative) values of calculated sensitivities indicate that the final concentration of Fus3* increase (decrease) with the increase of the parameter value.

The highest absolute value (-0,502 in model B and -0,651 in model C) has been calculated for parameter k_{91} that represents the positive feedback of Sst2 acting on the deactivation of Fus3*. Another parameter that has a great impact on the final concentration of the output is k_8 that represents the activation of Fus3. In model B, the final concentration of Fus3* is insensitive to the changes in parameter values: k_4 (hydrolisation of GαGTP into GαGDP), k_{41} (hydrolisation of GαGTP into GαGDP driven by Sst2*) and k_9 (deactivation of Fus3*). In model C, the final concentration of Fus3* is insensitive to the changes in parameter values: k_2 (deactivation of Ste2*), k_{41} and k_9.

All values of calculated sensitivities can be found in the appendix.

6 Discussion

The objective of the thesis was to suggest a model structure that is able to reproduce the experimental data from [Yu *et al.* 2008] and to explain the mechanism of the negative feedback. On the basis of previous knowledge about the mechanism of pheromone signalling system and taking into account the existence of a negative feedback of Fus3, many possible model structures were constructed. With the help of tool COPASI, parameters for all models were estimated on the base of experimental data. Four model structures were selected and presented in detail to give an overview. The results of parameter estimation were compared and discussed. On the base of AIC criterion, one model was chosen. The predictions of the selected model were presented as well as the parameter sensitivities were calculated. The following subsections discuss the results of this thesis.

6.1 Parameter estimation

It has already been mentioned in section 5.1.5 that the results of parameter estimation are not satisfying enough to ascertain that one of the proposed model structures give a clear answer how the negative feedback should look like in order to observe requested system dynamics at all considered levels of the pathway: "peak and decline" behaviour for Fus3 phosporylation, Ste5 membrane recruitment and G-protein dissociation while stimulation with only pheromone as well as a "constant after reaching a peak" behaviour for Fus3 phosporylation and Ste5 membrane recruitment and no change in the dynamics in the G-protein dissociation while stimulation with an additional inhibitor.

A possible reason of this situation could be an inadequate model structure. Although all models describe sufficiently the mechanism in wild type cells, they fail in describing the system dynamics in mutant cells during the stimulation with pheromone and inhibitor. It is not out of the question that the models are not

complex enough to provide an indisputable solution for the problem. Also some presumed initial concentrations may be misleading.

Another difficulty in evaluation of the results of the parameter estimation is the choice of the features that a certain fit has to possess so that it can be described as adequate and satisfying. It is hard to decide what is more important: the time when the peak occurs, the value of the steady state or the form of the curve. It is difficult to answer the question if a fit could be interpreted as an acceptable one if it has the right form and peak take places by the exact time, but it reaches a higher value of a steady state that expected what could be a result for an incorrect choice of the initial concentrations. Possibly, it would be useful to try different initial concentrations values.

6.2 Model selection

Model B has the minimal value of AIC that means that model B describes the dynamics of the processes with the most parsimony among all considered models. However, the AIC values for model D and model C are not significantly higher than the AIC value for model B.

6.3 Predictions of the model

The experimental data for the final concentration of not inhibited Fus3* as well as of inhibited Fus3* revealed that the inhibition of Fus3* evidently disrupts the dose-response alignment and reduces the sensitivity of the dose response. The calculated value of EC_{50} was reduced by about 20-fold in the given set of experimental data. The predictions of previously chosen model B do not correspond to the experimental results. Surprisingly, the predictions of model C are significantly better than the predictions of model B. The reason for this could be fact, that the predictions take only the final concentration of Fus3* for different pheromone concentrations into consideration and do not consider how the

dynamics of the discussed processes changes when the pheromone concentration vary. Therefore it would be misleading to ascertain that model C explains better the mechanism of negative feedback than model B.

6.4 Conclusion

Model B describes the dynamics of the system with the best accuracy and parsimony. This model contains three feedbacks. Sst2* promotes the dissociation of the complex into scaffold protein and Gβγ subunit. Sst2 mediates two different feedbacks. On of them promotes the hydrolisation of GαGTP into GαGDP and the second one promotes the deactivation of Fus3*.

There are three are conclusions that that can be drawn from this thesis and the whole project (in the thesis only the results of four models have been discussed, but more that 50 others have been tested and regarded). Firstly, Sst2* promotes the dissociation of the complex D instead of inhibiting the association of scaffold protein and Gβγ subunit. As next, the mechanism of the hydrolisation of GαGTP into GαGDP is less important because the output is insensitive to changes in parameters of this process. Lastly, the mechanism of the requested negative feedback is complex and consists of many feedback and, possibly, delays.

7 Outlook

There is an unquestionable need for further studies of the mechanism of the negative feedback in the pheromone pathway in yeast. A model that satisfactory reproduces the experimental data and generates correct predictions has still not been found. Many possible model structures with different complexity, different number and art of feedbacks have not been tested because of limited time for this project.

The finding of the exact mechanism of the Fus3-mediated feedback will supplement the previous knowledge about the pheromone signalling in yeast.

8 References

- Bozdogan H. (1987) Model selection and Akaike's Information Criterion (AIC): The general theory and its analytical extensions. *Psychometrika*, 52, 345-370.
- Burnham K.P. (2004) Multimodel inference: Understanding AIC and BIC in model selection. *Amsterdam Workshop on Model Selection*.
- Chasse S.A., Flanary P., Parnell S.C., Hao N., Cha J.Y., Siderovski D.P. & Dohlman H.G. (2006) Genome-Scale Analysis Reveals Sst2 as the Principal Regulator Mating Pheormone Signaling in the Yeast Sacharomyces cerevisiae. Eukaryotic Cell, 5, 330-346.
- Colman-Lerner A., Gordon A., Serra E., Chin T., Resnekov O., Endy D., Pesce C.G & Brent R. (2005) Regulated cell-to cell variation in a cell-fate decision system. *Nature*, 437, 699-706.
- Drogen van F., Stucke V.M., Jorritsma G. & Peter M. (2001) MAP kinase dynamics in response to pheromones in budding yeast. *Nature Cell Biology*, 3, 1051-1059.
- Hao N., Yildirim N., Wang Y., Elston T.C. & Dohlman H.G. (2003) Regulators of G Protein Signaling and Transient Activation of Signaling. *The Journal of Biological Chemistry*, 278, 46506-46515.
- Hayashi M. & Maeda T. (2006) Activation of the HOG pathway upon Cold Stress in Saccharomyces cerevisiae. *J. Biochem*. 139, 797-803.
- Hoops S., Sahle S., Gauges R., Lee C., Pahle J., Simus N., Singhal M., Xu L., Mendes P., and Kummer U. (2006). COPASI — a COmplex PAthway SImulator. *Bioinformatics,* 22, 3067-74.
- Kamrunnahar M., Braatz R.D. & Alkire C. (2004) Parameter sensitivity analysis of Pit Initiation at Single Sulfide Inclusions in Stainless Steal. *Journal of The Electrochemical Society*, 151, B90-B97.

- Kholodenko B.N. (2000) Negative feedback and ultrasensitivity can bring about oscillations in the mitogen-activated protein kinase cascades. *Eur. J. Biochem*, 267, 1583-1588.
- Klipp E. & Liebermeister W. (2006) Mathematical Modeling of intracellular signaling pathways. *BMC Neuroscience*, **7**(Suppl 1):S10.
- Klipp E., Herwig R., Kowald A., Wierling C. & Lehrach H. (2005) Systems Biology in practice. WILEY-VCH, 137-200.
- Kofahl B. & Klipp E. (2004) Modelling the dynamics of the yeast pheromone pathway. *Yeast*, 21, 831-850.
- Lorenz M.C. & Heitman J. (1997) Yeast pseudohyphal growth is regulated by GPA2, a G protein α homolog. *The EMBO Journal* 16(23), 7008–7018.
- Nazarko V.Y., Thevelein J.M. & Sibirny A.A. (2007).
- Qi M. & Elion E.A. (2005) MAP kinase pathways. *Journal of Cell Science*, 118, 3569-3572.
- Schaber J., Kofahl B., Kowald A. & Klipp E. (2006) A modelling approach to quantify dynamic crosstalk between the pheromone and the starvation pathway in baker's yeast. *FEBS Journal* 273, 3520-3533.
- Shao D., Zheng W., Qiu W., Ouyang Q. & Tang C (2006) Dynamic Studies of Scaffold-Dependent Mating Pathway in Yeast. *Biophysical Journal*, 91, 3986-4001.
- Shaw A.S. & Filbert E.L. (2009) Scaffold proteins and immune-cell signalling. *Nature Reviews Immunology* 9(1), 47-56.
- Wang Y. & Dohlman H.G. (2004) Pheromone Signaling Mechanisms in Yeast: A prototypical Sex Machine. *Science*, 306, 1508-1509.
- Yu R.C., Pesce C.G., Colman-Lerner A., Lok L., Pincus D., Serra E., Holl M., Benjamin K., Gordon A. & Brent R. (2008) Negative feedback that improves information transmission in yeast signalling. *Nature*, 456, 755-761.

Appendix

Equations:

Model	Equations	
0	$v_1 = k_1 \cdot Ste2[t] \cdot P$ $v_2 = k_2 \cdot Ste2^*[t]$ $v_3 = k_3 \cdot Ste2^*[t] \cdot G\alpha\beta\gamma[t]$ $v_4 = k_4 \cdot G\alpha GTP[t]$ $v_5 = k_5 \cdot G\alpha GDP[t] \cdot G\beta\gamma[t]$ $v_6 = k_6 \cdot C[t] \cdot G\beta\gamma[t]$	$v_7 = k_7 \cdot D[t]$ $v_8 = k_8 \cdot D[t] \cdot Fus3[t]$ $v_9 = k_9 \cdot Fus3^*[t]$ $v_{10} = k_{10} \cdot Fus3^*[t] \cdot Sst2[t]$ $v_{11} = k_{11} \cdot Sst2^*[t]$ $v_{12} = k_{12} \cdot Ste2^*[t]$
A	$v_1 = k_1 \cdot Ste2[t] \cdot P$ $v_2 = k_2 \cdot Ste2^*[t]$ $v_3 = k_3 \cdot Ste2^*[t] \cdot G\alpha\beta\gamma[t]$ $v_4 = k_4 \cdot G\alpha GTP[t]$ $v_5 = k_5 \cdot G\alpha GDP[t] \cdot G\beta\gamma[t]$ $v_6 = k_6 \cdot C[t] \cdot G\beta\gamma[t]$	$v_7 = k_7 \cdot D[t] + k_{71} \cdot D[t] \cdot Sst2^*[t]$ $v_8 = k_8 \cdot D[t] \cdot Fus3[t]$ $v_9 = k_9 \cdot Fus3^*[t]$ $v_{10} = k_{10} \cdot Fus3^*[t] \cdot Sst2[t]$ $v_{11} = k_{11} \cdot Sst2^*[t]$ $v_{12} = k_{12} \cdot Ste2^*[t]$
B	$v_1 = k_1 \cdot Ste2[t] \cdot P$ $v_2 = k_2 \cdot Ste2^*[t]$ $v_3 = k_3 \cdot Ste2^*[t] \cdot G\alpha\beta\gamma[t]$ $v_4 = k_4 \cdot G\alpha GTP[t] + \underline{k_{41} \cdot G\alpha GTP[t] \cdot Sst2^*[t]}$ $v_5 = k_5 \cdot G\alpha GDP[t] \cdot G\beta\gamma[t]$ $v_6 = k_6 \cdot C[t] \cdot G\beta\gamma[t]$	$v_7 = k_7 \cdot D[t] + \underline{k_{71} \cdot D[t] \cdot Sst2^*[t]}$ $v_8 = k_8 \cdot D[t] \cdot Fus3[t]$ $v_9 = k_9 \cdot Fus3^*[t] + \underline{k_{91} \cdot Sst2[t] \cdot Fus3^*[t]}$ $v_{10} = k_{10} \cdot Fus3^*[t] \cdot Sst2[t]$ $v_{11} = k_{11} \cdot Sst2^*[t]$ $v_{12} = k_{12} \cdot Ste2^*[t]$
C	$v_1 = k_1 \cdot Ste2[t] \cdot P$ $v_2 = k_2 \cdot Ste2^*[t]$ $v_3 = k_3 \cdot Ste2^*[t] \cdot G\alpha\beta\gamma[t]$ $v_4 = k_4 \cdot G\alpha GTP[t] + \underline{k_{41} \cdot G\alpha GTP[t] \cdot Sst2^*[t]}$ $v_5 = k_5 \cdot G\alpha GDP[t] \cdot G\beta\gamma[t]$ $v_6 = k_6 \cdot C[t] \cdot G\beta\gamma[t]$ $v_7 = k_7 \cdot D[t] + \underline{k_{71} \cdot D[t] \cdot Sst2^*[t]}$	$v_8 = k_8 \cdot D[t] \cdot Fus3[t]$ $v_9 = k_9 \cdot Fus3^*[t] + \underline{k_{91} \cdot Sst2[t] \cdot Fus3^*[t]}$ $\underline{v_{10} = k_{10} \cdot X^*[t] \cdot Sst2[t]}$ $v_{11} = k_{11} \cdot Sst2^*[t]$ $v_{12} = k_{12} \cdot Ste2^*[t]$ $\underline{v_{13} = k_{13} \cdot Fus3^*[t] \cdot X[t]}$ $\underline{v_{14} = k_{14} \cdot X^*[t]}$
D	$v_1 = k_1 \cdot Ste2[t] \cdot P$ $v_2 = k_2 \cdot Ste2^*[t]$ $v_3 = k_3 \cdot Ste2^*[t] \cdot G\alpha\beta\gamma[t]$ $v_4 = k_4 \cdot G\alpha GTP[t] + \underline{k_{41} \cdot G\alpha GTP[t] \cdot Sst2^*[t]}$ $v_5 = k_5 \cdot G\alpha GDP[t] \cdot G\beta\gamma[t]$ $v_6 = k_6 \cdot C[t] \cdot G\beta\gamma[t] + \underline{k_{61} \cdot C[t] \cdot G\beta\gamma[t] \cdot D[t]}$	$v_7 = k_7 \cdot D[t] + \underline{k_{71} \cdot D[t] \cdot Sst2^*[t]}$ $v_8 = k_8 \cdot D[t] \cdot Fus3[t] + \underline{k_{81} \cdot D[t] \cdot Fus3[t] \cdot Fus3^*[t]}$ $v_9 = k_9 \cdot Fus3^*[t] + \underline{k_{91} \cdot Sst2[t] \cdot Fus3^*[t]}$ $v_{10} = k_{10} \cdot Fus3^*[t] \cdot Sst2[t]$ $v_{11} = k_{11} \cdot Sst2^*[t]$ $v_{12} = k_{12} \cdot Ste2^*[t]$

Initial concentrations of the components

Component	Initial Concentration [μM]
Ste2	1.667
Ste2*	0
Gαβγ	1.667
GαGTP	0
GαGDP	0
Gβγ	0
C	0.036
D	0
Fus3	0.686
Fus3*	0
Sst2	0.505
Sst2*	0
X (only Model C)	0.1
X* (only Model C)	0

Estimated parameter values

Parameter	Model A	Model B	Model C	Model D
k_1	0,011	0,071	0,020	0,01
k_2	0,057	2,457	0	0,045
k_3	0,157	0,724	0,174	0,148
k_4	0,165	1,259	0,34	0,147
k_{41}	----	1,124	0	0,003
k_5	0,029	0,002	0,510	0,034
k_6	0,034	0,021	0,215	0,046
k_{61}	---	---	---	0,025
k_7	0,003	0,004	0,037	0,009
k_{71}	0,042	0,261	1,573	0,755
k_8	0,501	0,818	0,268	0,477
k_{81}	---	---	---	0,120
k_9	0,013	0	0	0,001
k_{91}	---	0,017	0,005	0,011
k_{10}	192,589	0,342	0,064	0,004
k_{11}	0,229	0,643	0,010	0,007
k_{12}	0,022	1,199	0,002	0,018
k_{13}	---	---	0,064	---
k_{14}	---	---	0,010	---

Calculated parameter sensitivities for all models

Parameter	Model A	Model B	Model C	Model D
k_1	-0.438	-0,018	-0,031	-0,171
k_2	0.099	0,012	-0,00001	0,123
k_3	0.190	0,084	0,237	0,163
k_4	-0.281	-0,00003	-0,085	-0,014
k_{41}	----	0,00033	0,004	-0,0001
k_5	-0,441	-0,194	-0,131	-0,162
k_6	0,126	0,334	0,444	0,373
k_{61}	---	---	---	0,002
k_7	-0,312	-0,079	-0,049	-0,067
k_{71}	-0,374	-0,262	0,367	-0,312
k_8	0,634	0,495	0,601	0,490
k_{81}	---	---	---	0,265
k_9	-0,937	-0,0000007	0,001	-0,014
k_{91}	---	-0,502	-0,651	-0,523
k_{10}	-0,270	-0,232	-0,357	-0,275
k_{11}	-0,009	0,232	0,373	0,289
k_{12}	-0,587	-0,100	-0,400	-0,314
k_{13}	---	---	-0,357	---
k_{14}	---	---	0,373	---

Acknowledgments

I am very grateful to Prof. Dr. Dr. hc. Edda Klipp who enabled me to write this thesis at the Group of Theoretical Biophysics at Humboldt University. I would like to thank Dr. Jörg Schaber for being my advisor, his patience and many valuable suggestions. I would also like to thank Prof. Dr. Hans-Peter Herzel and again Prof. Dr. Dr. hc. Edda Klipp for the examination of this thesis. Furthermore, I would like to thank all the members of the group for support and cooperation. Additionally I want to thank my family and my friends for supporting me.

Eigenständigkeitserklärung

Hiermit versichere ich, dass ich die vorliegende Bachelorarbeit selbständig verfasst und keine anderen als die angegebenen Quellen und Hilfsmittel verwendet habe.

Berlin, den 22. Oktober 2009

(Adriana Supady)